Suspended Particulate Dynamics in the Columbia River Estuary

Annika Merle Virginia Fain
B.Sc., Western Washington University, 1997

A thesis submitted to the faculty of the
Oregon Graduate Institute of Science and Technology
in partial fulfillment of the
requirements for the degree of
Master of Science
in
Environmental Science and Engineering

October 2000

The thesis "Suspended particulate dynamics in the Columbia River estuary" by Annika Merle Virginia Fain has been examined and approved by the following Examination Committee:

David A. Jay, Ph.D.
Associate Professor, Thesis Advisor

Antonio M. Baptista, Ph.D.
Professor

Patricia L. Toccalino, Ph.D.
Assistant Professor

Richard W. Sternberg, Ph.D.
Professor Emeritus

For my mother, Carolyn Joyce Fain

Acknowledgments

I thank my advisor, David Jay, for all his support and encouragement. I am grateful for all of the input he gave me on this thesis and throughout my work at OGI. I wish to thank the other members of the Jay lab (Phil Orton, Doug Wilson, Tobias Kukulka, Pradeep Naik, and John McGinity) for their support and suggestions. I also wish to thank Antonio Baptista, Mike Wilkin, Cole McCandlish, and Ed Myers for helping me obtain and interpret CORIE data. I wish to express my gratitude toward Richard Sternberg for sharing his expertise on sedimentology.

I am grateful to all the committee, including Patty Toccalino, for their helpful suggestions and comments that have helped improve my thesis. I wish to thank them all for taking time out of their busy schedules to serve on my committee.

I wish to thank many of the staff and students at OGI who have been encouraging and supportive over the past two years. Additionally, I wish to express the utmost gratitude to my older brother and friends for always being supportive and encouraging.

This work was funded by the Office of Naval Research AASERT grant, N00014-96-1-0893, and the National Science Foundation Grant *Columbia River Land-Margin Ecosystem Research Project*, OCE-9412928, and SGER, *Amplification of El Niño-Southern Oscillation (ENSO) Climate Effects in Estuaries*, OCE-9816083. Any opinions, findings, and conclusions or recommendations expressed in this material are those of the author and do not necessarily reflect the view of the Government, Office of Naval Research, or the National Science Foundation.

Table of Contents

List of Figures

List of Tables

ABSTRACT

Suspended Particulate Dynamics in the Columbia River Estuary

Annika Merle Virginia Fain, B.Sc.
M.S., Oregon Graduate Institute of Science and Technology
September 2000
Supervising Professor: David A. Jay

The purposes of this work were: a) to develop Acoustic Doppler Current Profiler (ADP) data analysis methods for the study of sediment dynamics, and b) to apply these methods to data from the Columbia River Estuarine Turbidity Maximum (ETM) over time scales ranging, from intra-tidal to seasonal. Sediment dynamics were investigated using velocity and acoustic backscatter (ABS) data from four long-term COlumbia River Estuary Observation and Forecast System (CORIE) ADP moorings and three seasonal 1997 Land Margin Ecosystem Research (LMER) shipboard surveys. ABS data were calibrated and converted to suspended particulate matter (SPM) by using SPM-ABS relationships determined from LMER data. Optical Backscatter Sensor (OBS) readings were used as an intermediary in calibration between ABS and gravimetric SPM pump samples.

A new inverse method was developed for quantifying sediment concentrations representing multiple settling velocity (W_s) classes from ABS-derived SPM. An inverse analysis in the form of a non-negative least squares optimization was used to estimate

sediment concentrations in four W_s-classes for each SPM profile. The inverse analysis method relies on W_s-spectra determined from Owen settling tube deployments, and uses concentrations associated with W_s-classes, not particle size, as the fundamental output. Calculated total SPM concentrations, W_s-specific concentrations, trapping efficiencies, along-channel velocities, and indicators of advection behavior were analyzed for each of four moored ADP stations on a variety of time scales.

The ETM was observed to migrate seasonally between the moored stations in a manner consistent with the LMER cruise observations. Variations in the W_s-class distribution and advection demonstrated that particle trapping was greatest during neap tides. Intra-tidal data show stronger advection on flood than on ebb tides, especially during periods of high stratification, e.g., the spring freshet. Additionally, advection appears to be greater on neap than spring tides. The combination of moored ADP ABS and velocity time series and *in situ* sediment characterization data provide a detailed spatial and temporal record of SPM processes in the Columbia River Estuary. The data processing approach developed here substantially advances the ability of estuarine scientists to provide dynamical insight into ETM processes. It has provided an unprecedented multi-time scale view of the Columbia River ETM.

CHAPTER 1

Introduction

The purposes of this work are a) to describe and understand suspended particulate matter (SPM) dynamics within the Estuarine Turbidity Maxima (ETM) over a range of time scales, and b) develop new data processing methods for moored Acoustic Doppler Current Profiler (ADP) time series and vessel data to make this possible. Acoustic technology provides the scientific community with potentially useful tools for measuring water velocity, sediment concentration, and sediment movement. Acoustic Doppler Current Profilers (ADPs/ADCPs) can provide both detailed vertical resolution and long records of velocity and acoustic backscatter (ABS). The potential for use of ADPs for interpretation of estuarine sediment dynamics has not been realized, however, because of difficulties in interpretation of suspended sediment properties in terms of acoustic backscatter. Definition of SPM concentration and flux fields from acoustic measurements must take into account the SPM balance characteristic of estuarine environments and the properties of the SPM itself. In particular, the presence of large aggregates prevents the direct application of Stokes law, which describes the settling velocity (W_s) for idealized, spherical particles, or scattering theory formulated for isolated particles.

The analysis approach employed here borrows elements of previous single frequency inverse methods for determination of SPM concentration (Lynch and Agrawal, 1991; Lynch et al., 1994). A single-frequency inversion has the advantage of using dynamical information present in SPM profiles. Results depend, however, on an assumed SPM dynamic balance of settling velocity and shear velocity. Previous studies have also often had to assume a W_s-distribution, and use Stokes Law to translate particle number

and W_s into particle diameter and concentration. For estuarine environments, where silt-sized particles often appear as aggregates of uncertain density, these procedures are disadvantageous. Also, W_s-classes (rather than size classes) have been used to avoid, unwarranted assumptions regarding the settling behavior of aggregates. Measured, rather than assumed, settling velocity spectra were used. As with previous single frequency inverse analyses (Lynch and Agrawal, 1991; Lynch et al., 1994; Lee and Hanes, 1995), a Rouse equation (a balance in the vertical between turbulent SPM flux and particle settling) has been used in this study. This approach omits advection. Unlike most previous studies, the importance of advection was evaluated and periods when advection may affect SPM properties were identified. Advection effects were found to be generally small to moderate. When advection was present, its effects were often counter-acted by stratification.

A novel scaling analysis and three parameters were used to describe ETM particle trapping processes. The three parameters are Rouse Number (P), Trapping Efficiecy (E) and Advection Number (A). All are relatively insensitive to calibration issues, can be determined routinely from moored instrument data, and provide insight into the behavior of the system as a whole. $P=W_s(kU_*)^{-1}$ is the Rouse number which describes vertical mixing and settling of particles. E is $C_mC_s^{-1}$, where C_m is the maximum SPM concentration (over six hours) in the ETM and C_s is the fluvial source concentration. A is $PH_m(H)^{-1}$, where H_m is elevation of maximum concentration, and H is total depth. A is robust, because it relies only on the assumption that SPM increases with increasing ABS or OBS. This is useful, because W_s-class distribution of SPM concentration and SPM transports change drastically with distance from the bed.

The Columbia River estuary resides in a valley incised into Tertiary volcanic rocks and sediment. It has a pronounced ETM due to particle trapping by strong tidal currents and a robust gravitational circulation (Jay and Musiak, 1994). The strength of its circulation is in part a response to topographic confinement. The tide is mixed

semidiurnal and diurnal with a tidal species number (the ratio of diurnal to semidiurnal constituents) of ~0.6 (Callaway, 1971).

There were five hypotheses tested in this study. They are related to the patterns of and relationships between supply, retention, and export of bulk SPM and W_s-class specific SPM over a variety of temporal scales. The hypotheses are:

H1: Fluvial SPM supplied during a freshet period is exported from the system primarily by spring tides during, and shortly after, the freshet.

H2: Peripheral bays serve as important reservoirs for storage of SPM on tidal monthly and seasonal time scales.

H3: Flood ETM events are typically more advective than ebb events, especially during periods of high stratification, i.e., on neap tides and during periods of high flow.

H4: Advection is more important for sediment transport on neap tides than spring tides.

H5: Trapping efficiency, E, is maximal during the lowest flow periods and exhibits significant spatial heterogeneity.

H3 and H4 are long standing hypotheses of the NSF-funded Columbia River Estuarine Turbidity Maxima Land Margin Ecosystem Research (LMER) Program, but had not yet been tested in a rigorous way.

The data uses in this study stem from two sources:

1. LMER staged ten cruises over the 1990-99 period to examine ETM properties. During these cruises a wide variety of biological, physical, and chemical data were collected, including: ADCP velocity and acoustic backscatter, Conductivity Temperature Depth profiler (CTD) data, grab samples of sediment, and sediment-water samples from a modified Owen Tube and comprehensive zooplankton data.

Three seasonal cruises took place between May 1997 and October 1997, providing important sediment characterization and calibration data for this study.

2. The COlumbia River Estuary Observation and Forecast System (CORIE) deployed four ADPs during late 1996 and early 1997. The four CORIE ADP moorings consisted of three in the South channel (Red26, Tansy, and Am169) and one in the North channel (Am012) (Fig. 1.1).

A combination of CORIE moored and LMER vessel data were utilized to understand ETM processes. The observations and data analysis in this thesis quantify in uprecedented detail the Columbia River estuarine sediment dynamics, which previously had been observed only intermittently during cruises.

The three chapters that follow provide a detailed examination of the seasonal, tidal-monthly and intra-tidal patterns of SPM movement in the Columbia River estuary (Chapter 2), present a more detailed examination of acoustic calibration procedure and the inverse analysis (Chapter 3), and provide a summary of results and future research ideas (Chapter 4).

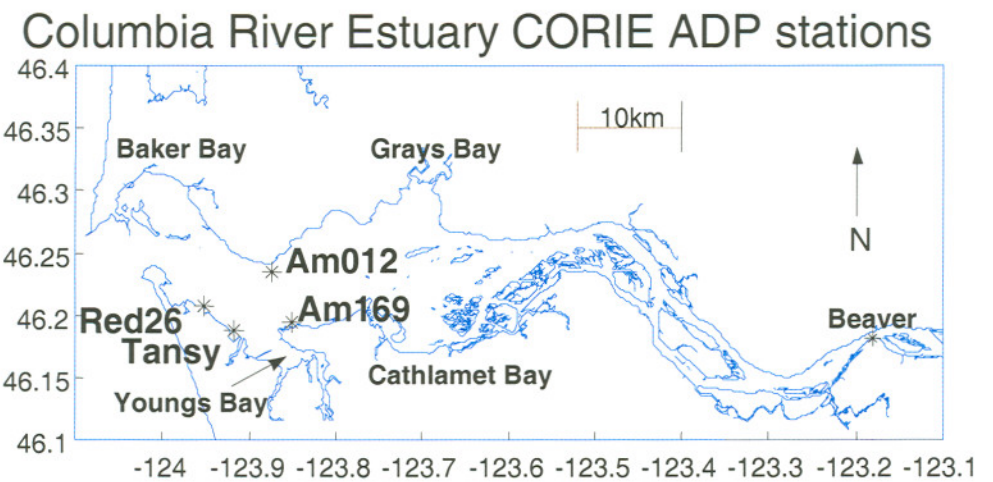

Figure 1.1. Map of Sontek moored Columbia River Estuary Observation and Forecast System (CORIE) ADP stations (*) in the Columbia River Estuary for 1997. Red26 and Am169 had 0.5 MHz ADPs, while Tansy and Am012 had 1.5 MHz ADPs.

CHAPTER 2[1]

Seasonal, Tidal-Monthly and Intra-Tidal Patterns of Particulate Matter Dynamics in a River Estuary

Abstract

We have investigated seasonal, tidal-monthly, and intra-tidal suspended particulate matter (SPM) dynamics in the Columbia River Estuary from May to December 1997 using acoustic backscatter (ABS) and velocity data from four long-term Acoustic Doppler Profiler (ADP) moorings in or near the Estuarine Turbidity Maximum (ETM). The ABS were calibrated and converted to total SPM concentrations by determining ABS-SPM relationships from three seasonal (May, July, and October) Land Margin Ecosystem Research (LMER) cruises, employing *in-situ* calibrated optical backscatter (OBS) as an intermediary. Four characteristic settling velocity (W_s) classes were defined from Owen Tube samples collected during the LMER cruises. A suspended particulate matter profile model was applied to the total ABS-derived SPM concentration. An inverse analysis, in the form of a non-negative least squares minimization, was used to determine the contribution of the four W_s-classes to each total SPM profile. The outputs from the profile model and the non-negative least squares inverse analyses are 6-8 month time-series of total and W_s-specific SPM concentrations, and transport at each

[1] submitted to Estuaries.

mooring at 0.25-0.50 m resolution from the free surface to 2-3 m from the bed. SPM dynamics were investigated using these time series along with sediment character and composition data. Three non-dimensional parameters were used to investigate how river flow and tidal forcing affect particle trapping: a Rouse number P (balance of vertical mixing and settling), a trapping efficiency E (ratio of maximum SPM concentration in the estuary to fluvial source concentration), and an advection number A (ratio of height of maximum SPM concentration to friction velocity). Results suggest the most effective particle trapping, E, occurs during neap tides with low river flows. The location of the ETM and the maximal trapping migrated seasonally in a manner consistent with the increase in salinity intrusion length after the spring freshet. Maximal A values occurred during highly stratified neap flood tides. These results could not have been achieved using either vessel or moored instrumentation alone. Thus, use of moored ABS, calibrated by cruise data, allows examination of estuarine sediment dynamics in the Columbia River Estuary with an unparalleled degree of temporal and spatial resolution.

2.1 Introduction

Estuaries are among the most productive parts of the world oceans and provide habitat for many shellfish and commercial fish species (Smith et al., 1991). Estuaries are also being altered globally by eutrophication, habitat loss, climate change, navigation, development, and pollution (LMER Coordinating Committee, 1992). It is vital, therefore, to understand the interaction of physical, chemical, and biological processes that promote and control estuarine productivity. A significant contribution to estuarine productivity occurs in the ETM, where organic detritus is assimilated into the estuarine food chain. In an ETM, SPM is concentrated and trapped, temporarily or permanently. SPM concentrations 10 to 100 times as large as adjacent regions are typical (Nichols and Biggs, 1985). This concentration of particles by circulation processes represents both a refuge from export and a food source for epibenthic organisms. While an ETM may accumulate material supplied from either the fluvial or oceanic environments, fluvial

material predominates in river estuaries like in the Columbia River estuary (Gelfenbaum, 1983).

ETM processes play a major role in a wide variety of estuarine ecosystems around the world, e.g., Chesapeake Bay (Thevenot and Krauss, 1993), the Hudson River estuary (Bokuniewicz and Arnold, 1984), the Gironde in France (Allen et al., 1990), the Tay estuary in Scotland (Weir and McManus, 1987), the Weser in Germany (Grabemann and Krauss, 1989), and the Columbia River estuary (Gelfenbaum, 1983; CREST, 1984). Though there are a wide variety of circulation processes that trap SPM to form an ETM, the mechanism having the greatest ecological significance, usually occurs near the head of salinity intrusion (Fig. 2.1). This ETM position represents a balance of landward transport of SPM near the bed by the tides and mean flow, fluvial SPM supply (sometimes augmented by the marine environment), and sporadic export events (Jay and Musiak, 1994). Lateral exchange with shallow areas sheltered from strong currents is an important process in some systems (e.g., San Francisco Bay, Lucas et al., 1999), and long-term deposition occurs in some but not all ETM regions. Because of its position near the head of the salinity intrusion, the ETM conforms to the same primary forcing factors as salinity intrusion itself: channel geometry, river flow, and tides. The character of the SPM supplied and timing of this supply from the basin provides additional constraints on ETM dynamics not applicable to salinity intrusion itself. Given this forcing, ETM processes can be expected to vary, not just tidally, but on time scales from intra-tidal to seasonal and inter-annual. Because of the difficulty of measuring SPM by size or W_s-class over long periods, it has not usually been possible to observe ETM processes over all relevant time scales (Grabbemann and Krause, 1989).

The purpose of this paper is to describe and understand ETM dynamics over a range of time scales from intra-tidal to seasonal. To resolve the methodological problems implied by these diverse time scales, we have used a combination of cruise measurements of SPM properties and moored Acoustic Doppler Profiler (ADP) measurements of velocity and acoustic backscatter (ABS). Total and settling velocity (W_s) class SPM concentrations were inferred from ABS via an inverse method, using cruise data for

calibration. We have used data from the COlumbia RIver Estuary Observation and Forecast System (CORIE-http://www.ccalmr.ogi.edu/CORIE; Baptista et al., 1998; Baptista et al., 1999) moored instrumentation records and Columbia River Estuarine Turbidity Maxima-Land Margin Ecosystem Research (CRETM-LMER) vessel observations to define ETM characteristics for 1997.

2.2 Experimental Site: The Columbia River Estuary

The Columbia River has a drainage basin area of 660,500 km^2 and an annual average river flow of approximately 7500 $m^3 s^{-1}$ (Fig. 2.2). It is the third largest river in North America. The arid eastern interior sub-basin, ~94% of the total basin area, supplies approximately 75% of the total basin runoff, primarily in the form of spring snow melt. The coastal sub-basin, ~6% of the total basin area, supplies 25% of the total river flow (Sherwood et al., 1990). The largest monthly average flows are observed during the May-June freshet period, due to snowmelt in the eastern sub-basin. Flows in the Columbia River are at present regulated by 18 main-stem dams and more than 100 dams on its tributaries (USACE, 1999). The river now provides an average of 9.7 million metric tons of sediment every year to its estuary, about half of the pre-regulation sediment load. Most of the sediment consists of coarse silt and fine sand carried in suspension (Simenstad et al, 1990).

The Columbia River estuary has pronounced ETM due to particle trapping by very strong tidal currents and a robust gravitational circulation (Jay and Musiak, 1994). The strength of these circulation processes is in part a response to topographic confinement. The Columbia River estuary resides in a valley incised into Tertiary volcanic rocks and sediment. The tide is mixed diurnal and semidiurnal with a tidal species number (ratio of diurnal to semidiurnal constituents) of ~0.6 (Callaway, 1971). The maximum tidal range is 3.6-4 m. Tidal influence can extend as much as 150 km upstream during low flow periods (CREST, 1984). The tidal maximum salinity intrusion length varies from about 15 to 50 km, depending on tidal range and river flow. Due to the

dominance of strong tides and river discharge, wind usually is a negligible forcing in the deeper channels of the Columbia River estuary (Jay and Smith, 1990; Sommerfield, 1999).

The estuary consists of two primary channels (Fig. 2.3). The North channel accommodates most of the tidal exchange and has a more marine character than the main, South channel. Salt transport usually is landward in the North channel and seaward in the South channel under a wide variety of flow conditions (Hughes and Rattray, 1980; Jay and Smith, 1990; Kay et al, 1996). The broad mid-estuary sand flats drain into the North channel, as do two large peripheral bays along the north side of the estuary, Baker Bay and Grays Bay. Another large bay, Youngs Bay, drains into the South channel in the ETM reach. Cathlamet Bay is a tributary to the South channel landward of the salinity intrusion. The arrangement of navigation structures is such that riverflow is supplied primarily to the South channel, which is also maintained for shipping through extensive dredging.

The ETM processes play a central role in the secondary productivity in the Columbia River estuary (Baross et al., 1994; Simenstad et al., 1994; Crump and Baross, 1996). Anthropogenic changes to the system, and to ETM processes, provide an incentive to examine SPM dynamics. Flow regulation, loss of peripheral wetlands, navigation channel construction, and channel maintenance have greatly altered natural circulation and sediment transport processes, with substantial impacts on the ETM and estuarine ecosystem it supports (Sherwood et al., 1990; Simenstad et al., 1992). Accumulation of organic pollutants and heavy metals in the ETM may also be an important factor affecting the ETM ecosystem (Hamblin, 1989).

Observations of turbidity, temperature, salinity, and sediment concentrations throughout the Columbia River estuary during the Land-Margin Ecosystem Research Program (LMER) show that there are three ETM in the Columbia River estuary (Jay and Musiak, 1994, 1996). One ETM is typically found near or seaward of the upstream limits of salinity intrusion in the South channel, 15 to 30 km from the ocean entrance. Another

ETM is found in the North channel near the upstream limits of salinity intrusion, at or seaward of Am012. The position of the North channel ETM is less variable with river flow than the one in the South channel, likely because river flow input to the North channel is rather indirect. Finally, a poorly understood and ecologically less productive ETM is occasionally found in the South channel near the entrance, 5-8 km from the ocean entrance at the end of flood. This research focuses on the ETM at or near the upstream limits of the salinity intrusion.

The mean sediment size of bed material in the Columbia River estuary is approximately 177 μm. Although mean size varies seasonally [spring-158 μm, fall-183 μm, and winter-200 μm], more than 99% of permanent bed material in the major channels is typically sand (Sherwood and Creager, 1990). Deposits of fine sediments, silts and clays, occur only in reaches isolated from strong tidal currents, especially in the peripheral bays. USGS data provided by D. Hubbell (US Geological Survey, personal communication) suggested that sand-sized material makes up approximately 45% of the total sediment load (Sherwood et al., 1990). During periods of high riverflow much of the finer sand travels in suspension. It has been estimated that the estuary retains at least seasonally about 30% of the material supplied to it for at least one year (US Geological Survey, 1971). The remainder is exported during high flow events and strong spring tides.

2.3 Scope of Research

The primary goals of this research were to a) gain a better understanding of ETM sediment dynamics over a wide range of time scales and b) develop the necessary tools to achieve this goal. These objectives were pursued using extensive data sets collected in the Columbia River estuary during 1997 through funding provided from the Office of Naval Research (ONR) and National Science Foundation (NSF). Data from four moored ADPs were provided by the ONR-funded CORIE observation and forecast system (Baptista, 2000) for the May to December 1997 period (Fig. 2.3). Three of the long-term stations

were in the South channel: from river to ocean, Am169, Tansy, and Red26 (Fig. 2.3). Additionally, one North channel station was studied: Am012. There were three LMER cruises during the observation period, in May, July, and December. Vessel results suggest that Tansy was in mid-ETM during the freshet season. After river flow declined in summer, the ETM was centered at or landward of Am169. In the North channel, the ETM was initially seaward of Am012. After the spring freshet, it was centered near Am012. However, all stations were likely within one tidal excursion of the ETM throughout the study.

The 1997 moored and cruise data are of particular interest for studying sediment dynamics because of a strong La Niña response in the Columbia basin which brought a cold winter, a very large snow pack, and the highest spring freshet flows since 1974. Also, the annual average discharge for water year 1997 was the highest in the Twentieth Century. The total sediment supply was well above average, about 18 million metric tons. The hypotheses tested relate to the supply, retention, and export of SPM on seasonal, monthly, and tidal scales. They were:

H1: Fluvial SPM supplied by a river during a freshet period is exported from the system primarily by spring tides during, and shortly after, the freshet.

H2: Peripheral bays serve as important reservoirs for storage of SPM on tidal monthly and seasonal time scales.

H3: Flood ETM events are typically more advective than ebb events, especially during periods of high stratification, i.e., on neap tides and during periods of high flow.

H4: Advection is more important for sediment transport during neap tides than spring tides.

H5: Trapping efficiency, *E*, is maximal during the lowest flow periods and exhibits significant spatial heterogeneity.

H3 and H4 are long standing but untested hypotheses of the LMER Project. They overlap to the extent that stratified, salt-wedge like floods are characteristic of neap tides, especially during the high-flow season.

2.4 Methods

2.4.1 Acoustic and Optical Background

Acoustic Doppler Profilers have been widely used to study estuarine circulation dynamics. They are attractive as a tool for analysis of SPM dynamics because they provide profiles of both water velocity and acoustic backscatter throughout most of the water column. Furthermore, ADPs with frequencies of 0.5 to 1.5 MHz are expected to be sensitive to the sand and large aggregates which dominate ETM processes (Schaffsma and Hay, 1999). ABS has been used in recent years to determine sediment concentration and transport in the laboratory and in a variety of environments (Young et. al, 1981; Lynch, 1985; Hanes et al., 1988; Libicki et al, 1989; Thorne et al., 1991; Crawford and Hay, 1993; He and Hay, 1993; Thevenot and Krauss, 1993; Lee and Hanes, 1996; Holdaway and Thorne, 1997; Hamilton, 1998; Shi et al., 1999). Also, ABS has been used to determine zooplankton concentration in pelagic environments where the biological contribution to ABS predominate over sediment contributions (Flagg and Smith, 1989; Barans et al., 1997; Ashjian et al., 1998). For measurement of either SPM or zooplankton with acoustical technology, proper calibration is essential in providing meaningful results. The considerable potential of ADP data as a source of information regarding ETM dynamics has not been realized because of difficulties in translating ABS into quantitative information regarding size or W_s-classes of SPM. We employ, therefore, a new approach described below.

ABS measurements have also been used in conjunction with OBS to study estuarine circulation (Thevenot & Krauss, 1993; Lynch et al., 1994; Green et al., 2000). OBS measurements are attractive in part because they have a wider dynamic range than

ABS sensors, and have been found to consistently provide a linear SPM-OBS relationship in the Columbia River estuary (Reed and Donovan, 1994). Furthermore, OBS provides a somewhat different measure of SPM concentration, one that responds most strongly to fine particles (Kineke and Sternberg, 1989; Ludwig and Hanes, 1990; Kineke and Sternberg, 1992; Orton, 1996; Battisto et al., 1999). Nonetheless, there is a strong overlap in the sensitivities of the instruments to SPM in the estuarine environment (Thevenot and Krauss, 1993) and both respond to the aggregates that dominate ETM dynamics in the Columbia River estuary. In the present study, ABS provides long-term SPM concentrations throughout the water column, while OBS plays a crucial role in intercalibration of sensors during cruises.

Understanding ETM dynamics requires defining the time histories of both total SPM and individual W_s-classes as a function of depth. To obtain multiple size class information from a single acoustic frequency, a SPM conservation law (a modified Rouse balance here) has been assumed, and applied in the inverse analysis method. The inverse analysis method of separating size or W_s-classes has been employed in both laboratory and marine contexts (Thorne et al., 1991; Lynch and Agrawal, 1991; Lynch et al., 1994; Lee and Hanes, 1995). Because estuarine SPM occurs largely in the form of flocs, scattering as a function of particle size cannot be assumed. We therefore employ mass concentration in W_s-classes, not size classes, as the output from our inverse analysis.

2.4.2 Instrumentation

The four long-term moored CORIE ADPs provide time series of both velocity and, after calibration, total SPM concentration. Two frequencies of bottom moored, upward looking Sontek ADPs were used to obtain water velocity and ABS data: 500 kHz (three-beam) instruments at Tansy and Am012, and 1.5 MHz (four-beam) instruments at Red26 and Am169 (Table 2.1). For the four-beam instruments, ABS from the vertical beam was used to determine SPM. ABS from a single (slant) beam was used for the three-beam instruments. Seasonal cruise OBS, CTD data, Owen Tube, and gravimetric

analyses were used in the calibration of the four moored ADP's. As expected with ADPs, horizontal velocity and ABS from slant beam were invalid near the surface of the water, resulting in loss of one to two bins of data. The vertical beam ABS data were valid, however, up to the bin just below the free surface.

2.4.3 Calibration of Optical Backscatter to SPM

OBS data were used as an intermediary in the calibration of moored ABS to SPM concentration following Thevenot and Krauss (1993). The OBS sensors employed for these purposes were calibrated in the laboratory by the manufacturer at the beginning and end of the field season. SPM was determined from gravimetric analysis of pumped samples. Field calibration curves were developed for each seasonal LMER cruise through linear regression of OBS vs. SPM concentration. The slope of the regression lines varied seasonally between 1.8 and 2.1 mg $(l\ NTU)^{-1}$. R^2 values were between 0.86 and 0.92. Both the linearity and seasonal variability are characteristic of the SPM vs. OBS relationship of cruises conducted over the 1990-1999 period (Reed and Donovan, 1994). Once an OBS vs. SPM relationship was determined from cruise data, OBS profiles taken within approximately 50 to 100 m of each of the mooring locations were used in the calibration of moored instrument ABS.

2.4.4 Calibration of Acoustic Backscatter

A meaningful determination of SPM concentration from ABS requires correction of the raw signal and calibration against an external standard. At each step, the frequency of the instrument must be considered. Regression lines of ABS vs. SPM (determined from OBS) were developed for all stations. The slope of the regression line varied from 0.90 to 1.09 mg $(l\ dB)^{-1}$. R^2 values of between 0.40 and 0.60 were obtained. The distances between the vessel OBS and the moored ABS observations caused some of the scatter. Another factor was depth variability between sample locations.

Pre-processing converts ABS data from counts to dB; the conversion is weakly dependent on instrument frequency. Corrections for beam spreading, water column and sediment absorption, and the near-field non-linear effects (Fig. 2.4) were implemented (Libicki et al, 1989; Thorne et al, 1991; Osborne et al. 1994; Downing et al, 1995; Lee and Hanes, 1995; Hamilton, 1998; Hamilton et al., 1998; Deines, 1999). The most significant correction is the signal strength decay due to beam spreading and water column sound absorption, which varies strongly with instrument frequency and weakly with salinity. Details of these procedures and of the near-field correction are given in Chapter 3.

All ADPs except Am169 were affected during the late summer by biofouling (Table 2.1), which reduces the ABS without (in the present case) affecting the velocity signal. In addition, short gaps in the data were produced at some stations by failure of the telemetry or other instrumentation problems (Sommerfield, 1999). Internal characteristics of the data and CORIE maintenance records were used in determining which data should be excluded from the analysis.

2.4.5 Settling velocity classes

During the CRETM-LMER cruises, a Braystoke Sk-110 water sampler (modified Owen Tube) was deployed ~1 m above the bed every two hours (Reed and Donovan, 1994). Subsamples were taken from the bottom of the tube at eight designated time intervals. The settling velocity data for all 1997 seasonal cruises was examined to determine which W_s-classes were characteristic. The data were partitioned by season, tidal monthly occurrence (spring, neap) and by tidal phase (flood, ebb). While there was some variability between categories with regard to relative concentrations, there were no significant seasonal or tidal monthly trends in the identity of the dominant W_s-classes. The following four W_s-classes, designated C_1 to C_4, were found to be representative of the LMER data set as a whole, and were used in the inverse analysis: 0.014 mm s^{-1}, 0.3

mm s^{-1}, 2.0 mm s^{-1}, and 14 mm s^{-1}. Given a broad response of all W_s-classes in the inverse analysis: C_1 is "washload" (clay to fine silt), C_2 is medium to coarse silt, C_3 is fine aggregate material, and C_4 contains sand and large aggregates.

2.4.6 SPM Profiles and Scaling of SPM Conservation Equation

The inverse method used to convert each total SPM profile to a sum of W_s-class specific profiles requires that a predicted profile, matched to ambient hydrographic conditions, be determined for each settling velocity class. The approach employs a simplification of the mass conservation equation for SPM commonly known as the "Rouse Balance." The use of the dynamical balance in the presence of advection is justified through a scaling analysis. Derivation of settling-class specific profiles begins from the SPM conservation equation:

$$\frac{\partial C_i}{\partial t} = -\left(u\frac{\partial C_i}{\partial x} + v\frac{\partial C_i}{\partial y} + w\frac{\partial C_i}{\partial z} \right) + \frac{\partial\left[K_s \frac{\partial C_i}{\partial z} \right]}{\partial z} + W_{si}\frac{\partial C_i}{\partial z} \qquad (2.1)$$

where: C_i is concentration of the i^{th} settling class; t is time; z is height above bed; u and v are horizontal velocities; w is vertical velocity; K_s is vertical sediment diffusivity; W_{si} is settling velocity of the i^{th} settling class; and x and y are horizontal coordinates.

We assume here that the flow is laterally uniform and that mean vertical velocity w is small relative to W_s. Scaling of the SPM conservation equation results in the following non-dimensional mass conservation equation:

$$\pi\frac{\partial C_i}{\partial t} + A\frac{\partial C_i}{\partial x} = P_i\frac{\partial C_i}{\partial \sigma} + \frac{\partial}{\partial \sigma}\left[K_s \frac{\partial C_i}{\partial \sigma} \right] \qquad (2.2)$$

Where: $\pi = \omega H (k U_*)^{-1}$; $P_i = W_{si} (k U_*)^{-1}$; $A = H \Delta U (L_s k U_*)^{-1} = P_i H_m H^{-1}$; $L_s = \Delta U H^2 (H_m W_{si})^{-1}$ is a typical scale length for an ETM (defined as the horizontal distance over which SPM would settle from elevation H_m to the bed); U_* is the shear velocity close to the bed; ω^{-1} is the semidiurnal time scalar ($\omega = 1.4 \times 10^{-4}$ s^{-1}); $\sigma = z\ h^{-1}$ is the non-dimensional distance from the bed; H = ~15 m is scale depth; k =0.408 is Von Karman's constant (Nowell, 1983); ΔU =~1 m s^{-1} is the scale for the lower-layer velocity difference that drives sediment advection; and H_m = ~5 m is a scale depth for the maximum distance off the bed that high SPM concentrations exhibit during advective episodes. Lynch et al. (1991) were the first to use H_m/U_* as an indicator of advection.

The Rouse number scales settling vs. vertical mixing. For large aggregates, $P_4 = W_{s4} (k U_*)^{-1}$, varies between ~1 and 5. P_3, the Rouse number for small aggregates, varies between ~0.2 and 0.7. These values indicate that settling, along with vertical mixing, is a dominant ETM process. We examine below values of P_4 that are characteristic of periods of SPM retention and export.

The advection term is scaled by the advection number $A = P_4 H_m H^{-1}$. Since $H_m H^{-1}$ is at most O (1/3), A is typically smaller (~0.1 to 0.6) than the dominant settling and vertical mixing terms in (2.2), but may not be negligible. In fact, ETM formation would not occur if advection and spatial gradients were completely absent. While we do not include advection in our profile equations, we do use our results to understand when it might be important. Note in this context that A is robust parameter on which to base analyses, because it is independent of the inverse analysis and any specific ABS vs. SPM calibration. Calculation of A relies only on the assumption that SPM increases with increasing ABS or OBS. Finally, the acceleration term is scaled by $\pi = \omega H (k U_*)^{-1}$, where U_* = ~0.02 ms^{-1} is the average shear velocity at CORIE ADP stations and π is O (0.1), small enough to be neglected throughout.

Eq. (2.2) yields a balance of vertical mixing and settling, if acceleration and advection are neglected. This form has P_i and σ as the two non-dimensional parameters

and was the basis for the SPM profiles used in the inverse analysis. To calculate profiles, Eq. (2.2) is integrated once (assuming a no-flux condition at the free surface and at the bed, z_i=z_1, the non-dimensional concentration is equal to one.) to give:

$$-P_i\, C_i(\sigma) = K_S(\sigma)\frac{\partial C_i(\sigma)}{\partial \sigma} \tag{2.3}$$

One representation of the non-dimensional neutrally-stratified eddy diffusivity is (Long, 1981; Nowell and Long, 1983; Beach and Sternberg, 1988):

$$K_S(\sigma) = kU_*\sigma e^{-\sigma/L} \tag{2.4}$$

where scale depth L is approximately 1/3 of the total depth. U_* was estimated from near-bed velocity in the lowest ADCP bin using the drag coefficient (C_d) formulation:

$$U_* = v_{z_1}\sqrt{C_d} \tag{2.5}$$

Where v_{z_1} equals the velocity in the lowest bin and z_1 is the elevation of the lowest bin; z_1 was 1.8 m for 1.5 MHz ADPs and it was 2.7 m for 0.50 MHz ADPs. A C_d of 1.0 x 10^{-3} was used in both cases. The flow is typically stratified, and this value of C_d was chosen to account for the reduction of bed stress by density stratification (Giese and Jay, 1989). Equation 2.3 was solved numerically for each time and each mooring with a fixed W_s and a time-variable U_*. The scale concentration C_{1i} for each settling class is determined in the inverse analysis procedure.

It is important also to consider the potential effects of density stratification and advection on SPM profiles. Ideally, the eddy diffusivity profile would have been corrected for density stratification, but the necessary density data were not available for the moored instrument records. Stratification has been inferred qualitatively from the ADP velocity profiles and more directly from LMER cruise data. LMER cruise data

indicates that during times of high riverflow, a strong salt wedge occurs both on neap and spring tides. Low riverflow periods exhibit a salt-wedge-like salinity intrusion on neap tides, but weak stratification on spring tides. If stratification were systematically trapping SPM near the bed during neap periods of high stratification, we would expect an increase in the SPM gradient near the bed. This would cause the inverse analysis to predict that the fastest settling material (class C_4) was dominant on neap tides. In fact, the reverse is the case; the predicted amount of C_4 decreases on the neaps.

The likely reason for the apparent lack of stratification effects on SPM profile shape is that stratification and advection have opposing effects on an ETM and tend to occur together. That is, stratification tends to trap resuspended material near the bed, whereas advection tends to raise the level of maximum SPM concentration (H_m) up off the bed. Qualitative observations during LMER cruises further suggest that advection is most important during periods of high stratification; i.e., during salt-wedge advances on flood and slow erosion of the salt water mass on stratified ebbs. These ideas concerning advection are tested below.

One of the most important factors to determine about the ETM is the efficiency with which it traps particles, and the dependence of this trapping efficiency on external parameters. The trapping efficiency, E, is defined as the ratio of maximum ETM concentration of large particles to an external source concentration of small particles (those that may be aggregated in the ETM). This concept is based in part on mass conservation considerations. Jay and Musiak (1994) argued that trapping of large particles in an ETM is brought about by temporal correlations between SPM stratification and velocity shear at all tidal and sub-tidal frequencies. Since SPM is concentrated near the bed, flow processes that cause landward flow near the bed will be effective in trapping SPM. Relevant processes include subtidal gravitational circulation, tidal salt wedge advance, and internal asymmetry at overtide and subtidal frequencies. River flow provides the material to be trapped, but is not directly involved in particle trapping because it removes as much material as it supplies.

Fluvial source concentrations (in the denominator of E) were taken as fluvial SPM concentration as predicted from a model (Jay and Naik, 2000), based on 1963-1969 data provided by the US Geological Survey (US Geological Survey, 1971). The concentration of material trapped (in the numerator of E) was judged by the maximum concentration near the bed over a 6-hr period of the three largest W_s-classes from the inverse analysis ($C_2 + C_3 + C_4$), minus the calculated sand concentration determined by calculating the predicted bedload concentrations (more detailed discussion in 2.4.7). These three W_s-classes contain medium-coarse silt (C_2) and a range of aggregates ($C_3 + C_4$), which dominante the ETM processes.

2.4.7 Sediment Transport Equations and Parameters

An important issue in interpretation of the inverse analysis results is the identity of the rapidly settling material placed in class C_4 by the inverse analysis. LMER cruises have found that both sands typical of mid-estuarine channels and large flocs settle at about 14 mm s^{-1} (Reed and Donnovan, 1994). We would like to know, then, how much of the SPM observed in the C_4 settling class might actually be sand rather than aggregate. One way to judge the importance of ETM advection is to note when the concentration of C_4 is larger than could possibly be generated by resuspension, supposing that the bed was 100% covered by aggregates. We calculated, therefore, hypothetical sand and aggregate concentrations corresponding to the largest W_s-class, C_4. It should be noted that this approach leads to a very conservative evaluation of A, because the permanent bed is ~99% sand, and fines are only transiently present on the bed in the ETM reach.

The approach employed here to calculate sediment resuspension follows that outlined by Smith and McLean (1977), with some modification of the parameters to accord with more recent studies (Glenn and Grant, 1987; Beach and Sternberg, 1988; Vincent and Green, 1990; Fredsoe and Deigard, 1992; Wright, 1995; Sternberg et al., 1999). In this approach, a reference concentration of sediment , ϵ_a, is estimated at the top of the bedload layer at elevation z_a, for both sand and aggregates:

$$\varepsilon_a = \frac{\varepsilon_b \gamma_o S}{1+\gamma_o S} \tag{2.6}$$

with

$$S = \frac{\tau_b - \tau_c}{\tau_c} \tag{2.7}$$

where ϵ_b, volume concentration of the bed, is equal to 0.65 (assuming porosity of 0.35) and γ_o is a coefficient of proportionality assumed here to be equal to 2.0 x 10^{-5} (Drake and Cacchione, 1989). The concentration of SPM higher in the flow is then determined from ϵ_a, which incorporates the critical bed shear, τ_b, and the critical shear stress, τ_c, values (Table 2.2). The critical shear velocity was determined by using a formula from Middleton and Southard (1984). Shear velocity at ~2.0 m was used as U_* total and then we determined U_{*sf}, skin friction velocity, at the top of the bedload layer, assuming rounded bedform crests of height 0.4 m, unseparated flow, and a C_d of 0.840 (Smith and McLean, 1977). τ_c values were determined at the bottom bin depth for each W_s-class assuming a specific gravity for sand of 2.65 and for flocs of 1.02 (Table 2.2). The sand was assumed to have a diameter of 125 μm, in agreement with the observed average size during high flow conditions. The aggregate diameter was determined following Sternberg et al. (1999) from:

$$W_s = 0.0002(D)^{1.54} \tag{2.8}$$

where D is the elliptical nominal diameter.

2.4.8 Inverse Analyses Method

The purpose of the inverse analysis is to represent each observed SPM profile (as determined from ABS) as a sum of profiles for the four settling classes C_1 to C_4. Each settling class profile is in turn determined by a solution to the modified Rouse balance

(2.4), using a U_*, and a K_s profile determined by ambient conditions. The inverse analysis is implemented using a non-negative least squares algorithm (Lawson and Hanson, 1974; Menlke 1989; Lynch and Agrawal, 1994; Shen and Lemmin, 1998). The output of this inverse analysis is a value for each dimensional scaling concentrations, C_{1i}, for each time and station, providing profiles of C_1 to C_4 concentrations throughout the water. Methodological details and verification of inverse analysis are described in Chapter 3. Examples of the inverse analysis results for Am169 and Tansy are shown in Fig. 2.5a and 2.5b. Low passed versions of the modeled washload (C_1) and ETM material (C_2+C_3+C_4-sand) are shown in Fig. 2.6 for all stations. Sand has been excluded from the ETM material because aggregates dominate the ETM processes in the Columbia River estuary.

C_1 to C_4 on average contained 4.4 %, 26.4 %, 35.6 %, 33.6 % of the total material by weight, respectively in the Owen Tube analysis. The comparable percentages of the results of the inverse analysis for the moored ADP data, bottom bins, are 2.5 %, 28.3 %, 24.0 %, 45.2 %. Thus, there is close agreement between the Owen Tube and the inverse analysis regarding the total near bed percentage of fines ($C_1 + C_2$) and aggregates plus sand ($C_3 + C_4$). There is also good individual agreement for the classes C_1 and C_2. This close agreement between the Owen Tube and the inverse analysis for the fine settling classes likely affects the relatively uniform distribution in the vertical of C_1 and C_2. The inverse analysis over-estimates the amount of C_4, even though the bottom ADP bin is above the minimal Owen Tube. There are several possible reasons for this disagreement for classes C_3 and C_4: a) uncertain and variable Owen Tube depth, especially during periods of strong currents when C_3 and C_4 concentrations are large, b) systematic bias produced by the presence of both sand and aggregates in C_4, c) uncertainties in the near-field corrections for the ABS (Fig. 2.4 and Fig. 2.5), and d) the size dependece of the acoustic response to particles in a near Rayleigh scattering regime.

2.4.9 Sediment Transport and Residence Time Index

Bulk SPM transport was determined at all the stations as the product of bulk SPM and velocity at each station. W_s-class specific SPM transports for each time and level were also determined by multiplying the settling class concentrations by the observed velocities. The small W_s-classes, C_1 and C_2, are dominant at the surface throughout the record, and the surface SPM represent primarily the movement of small particles. The larger W_s-classes, C_3 and C_4, are dominant near the bed; therefore, the near bed transport calculations represent the movement primarily of larger particles.

A residence time index (R_T) was developed in order to understand SPM retention time in the system. R_T calculations were done for each channel, by estimating from inverse analysis results the integral amount of SPM in the ETM (as defined in Fig 2.3), and then dividing by the predicted fluvial SPM flux. R_T is only an index rather than a true residence time, because we cannot determine the volume of material stored on the bed, and because the system is not in a steady state. Additionally, the thickness of the layer of all the SPM in the ETM would make on the bed at neap tide was determined if the entire maximum SPM volume in the ETM were all deposited on the bed. The thickness was determined by using an average surface area, maximum concentration, and water-sediment interface density ranging from 180 kg m^{-3} to 270 kg m^{-3} (Winterwerp et al., 1993).

2.4.10 Methodological Concerns

One potential concern in the use of ABS for the measurement of SPM concentration is the presence in the ETM region of a large population of zooplankton with a size range similar to that of large aggregates (500-1,500 μm). We cannot exclude

occasional contamination of our results by backscatter of biological origin, but systematic investigation of the temporal and spatial distribution of zooplankton suggest several reasons why this is a minor factor in the present data set:

- Zooplankters and SPM have similar residence times, but the total annual zooplankton production, estimated to be <2,000 t (metric tons) for 1980-81 (Simenstad et al., 1990), is quite small relative to SPM supply, $>10^7$ t for 1997.
- The zooplankton population is dominated by an epibenthic organism (*Eurytemora affinis*) that is found in greatest numbers close to the bed below the lowest ADP bin (Morgan et al., 1997).
- The absolute numbers of zooplankton are small relative to the number of flocs. A systematic 8 d time series at several depths in mid-ETM in May 1995 found a median of 2.2×10^4 zooplankters m^{-3}, with maximum numbers of 5×10^5 m^{-3} (CRETM-LMER, 2000). This count is very small relative to the number of flocs, approximately 1.5×10^7 particles m^{-3}, inferred to be present from Owen tube results and floc density estimates.
- The tidal phase of maximum observed ABS is indicative of SPM. Near-bed ABS is largest at or shortly after the times of peak bedstress, a pattern appropriate to SPM, not epibenthic organisms (*Eurytemora affinis*). Epibenthic organisms, such as *Eurytemora*, migrate into the water column at times of low current velocity. Harpacticoid copepds are also present, however, and may be resuspended in the SPM at times of high bedstress.
- The largest observed ABS values occurred during the spring freshet, when zooplankton numbers were low (CRETM-LMER, 2000). The lowest ABS values were found during the summer and fall period when zooplankton populations reach their seasonal peak.

Finally, interpretation of the inverse analysis results must be carried out with the recognition that SPM transport processes exhibit substantial across-channel variability that cannot be defined from the moored instrument records. Stations Am012 and Am169

are located in the deepest part of the thalweg and likely exhibit greater landward transport than seen elsewhere at these cross-sections. For example, seaward transport along the north bank of the North Channel ~200 m north of Am012 has been documented from vessel observations (Jay and Musiak, 1994). Ebb currents and bank erosion are strong at Red26; vessel observations suggest that more landward transport occurs along the north side of the South Channel at this location. Tansy is located at the outside of a curve, and upstream bottom flow is absent except during neap tides. Extensive dredging between Tansy and AM169 suggests, however, that landward flow also occurs along the north side of the channel here.

2.5 Results

The result of the inverse analysis was a half-hourly time series of C_1 to C_4 profiles, in addition to those for total SPM and along-channel velocity. For closer examination of neap-spring and seasonal fluctuations, a low-pass Kaiser filter (Kaiser, 1974) was applied to all time series. The filter removed daily tidal oscillations but preserved neap-spring fluctuations for all moored ADP data from 1997. The four stations provide extensive SPM data and, via the inverse analysis, W_s-class distributions as a function of time. These results augmented by vessel and auxiliary data allow us to investigate the amount and composition of SPM supplied to and contained in the ETM. Examination of these patterns provides insight into ETM processes on time scales from intra-tidal to seasonal.

2.5.1 Seasonal and Tidal Monthly Patterns

It is convenient to consider seasonal and tidal monthly variability together, because the length of the available time series is not sufficient to cleanly separate these time scales, and because processes on the two scales interact. Seasonal variations in SPM concentrations and fluxes are driven primarily by river flow, either directly or through the

influence of river flow on estuarine circulation (Fig. 2.7). The tidal monthly variations in ETM processes are primarily driven by variations in tidal range. The tidal monthly part of the spectrum is also affected by the river flow record, which contains a weekly power-peaking cycle (related to hydroelectric operations) and natural variability at periods of less than one month. The strongest spring tides occur in mid-summer and mid-winter, but total bedstress is influenced by river flow as well as tidal currents. Maximum bedstresses occurred during the spring freshet (~d. 130), with a secondary peak at about d. 230 (Fig. 2.8).

The spring freshet of 1997 occurred from late April to mid-June with flows of 13 to 17 x 10^3 m^3 s^{-1} (Fig. 2.7). The SPM input to the system strongly varies with river flow Q_R; i.e., as ~$Q_R^{2.5}$ (Jay et al., 1999). Thus, most SPM input occurred during the spring freshet, and following winter storms not observed during this study. However, high SPM concentrations in the estuary and export events continue into July and August (Fig. 2.9 and 2.10), after the flow decreased to summer levels. The total transport for all stations (Fig. 2.10) supports H1 by demonstrating that SPM supplied during the spring freshet is exported primarily by spring tides, during and for about a month after the spring freshet.

The maximum predicted fluvial sediment supply during the study was on the order of 2.5 x 10^3 kg s^{-1} and maximum predicted sand transport was on the order of 1.3 x 10^3 kg s^{-1} (Fig. 2.7). The total SPM supplied during the March to June period was 12.7 x 10^6 t, out of the total water-year supply of 18.3 x 10^6 metric tons. Considerable SPM was also supplied by a high flow period in early January, during which the highest daily flows of the year were observed (~20,000 m^3s^{-1}) (USGS, 2000). It is not known, however, the degree to which material supplied during winter 1996-97 affected SPM dynamics during the May to December 1997 period. Summer river flow and sediment supply were unusually high, because of the very large snowpack during the winter of 1996-1997. The minimum seasonal flow was 3,849 m^3s^{-1}, >25% above the usual fall minimum of 2,500-3,000 m^3 s^{-1}.

The strength of the spring freshet flow is very evident in the ADP velocity record, e.g., at Red26, where bottom flow is absent or weak before d 190 (Fig. 2.11). Total SPM determined from ABS is maximal during after the spring freshet (Fig. 2.11), generally following the seasonal river flow and predicted SPM supply patterns shown in Fig. 2.7. The SPM time history indicates a limited residence time for SPM in the system, as well as a close linkage between the river and estuary. Total and W_s-class SPM, however, show strong neap-spring (tidal monthly) fluctuations not seen in Fig. 2.7, and elevated SPM levels continue for one to two months (depending on the station) after the end of the freshet. Furthermore, spring tide SPM levels are elevated throughout the record, suggesting an estuarine source of material. Given that storage of fines in the deeper channels is minimal due to strong currents, it is likely that high spring tide SPM values after the freshet result from storage of fines in peripheral areas, an idea we will return to.

The seasonal location of the ETM in the Columbia River estuary is evident from examination of the distribution of material trapped in the ETM, over time at the various stations (Fig 2.6). We focus first on processes in the South channel, where multiple stations make the influence of river flow on ETM position and concentrations evident (Fig. 2.6b). Until the end of the spring freshet at ~d 170, concentrations of the trapped material are at a seasonal maximum at all three South channel stations, but greatest at Tansy. This is consistent with shipboard observations that the ETM was centered near Tansy, but advected tidally from Red26 to Am169. As the flows decrease (d 170 to d 280), the order of concentrations is (from high to low): Am169, Tansy, and Red26. This pattern is consistent with the expected seasonal pattern of landward ETM migration to the vicinity of Am169.

In a normal flow year, the ETM would be found landward of Am169 from about August to October, but it is doubtful that this occurred, given the relatively high flows during summer and fall 1997. At the end of the record, there is an increase in the concentration of trapped material at Tansy, but not at Red26. This may be indicative of an increase in supply of sediment from lower river tributaries, not included in the flow time series of Fig. 2.7, or it may indicate increased resuspension from tributary bays due

to storms. That these patterns of ETM movement are subtle and, in the absence of a long history of vessel observations, perhaps subject to alternative interpretation, is indicative of the fact that all three stations are within the tidal excursion of the ETM throughout the time period. Also, exchange of material with Youngs Bay (between Tansy and Am169) may affect SPM values at those stations. Additionally, SPM concentrations at Red26 may be influenced by the near-mouth ETM, about which very little is known.

One of the most dramatic features of the low passed concentration records is that the highest SPM concentrations are found throughout the record at the North channel station, Am012 (Fig. 2.6c). Strong ETM trapping in the North channel is likely related to salt transport patterns in the system. Observations show that salt is transported landward under most hydrographic conditions in the N. Channel (Hughes and Rattray, 1980; Jay and Smith, 1990; Kay et al., 1996), whereas salt transport in the South channel is consistently seaward. Inferred, but unmeasured, is a salt transfer across the mid-estuary flats via shallow channels that trend a southeasterly (landward) direction from station Am012. In a similar manner, presence of landward SPM transport is consistent and strong near the bed in the North channel (Fig. 2.10d). During the spring freshet, Am012 is the only station that shows any landward bottom SPM transport, while surface transport at Am012 is only weakly seaward throughout most of the record. Even allowing for seaward SPM transport elsewhere in the section, it is likely that SPM, unlike salt, is neither transferred from the North to the South channel nor exported as regularly as in the South channel. This would allow larger particles to accumulate in the North channel, with possible long-term storage in the two peripheral bays that are known to be accreting (Sherwood et al., 1990).

Sediment transport for two spring tides both during and shortly after the spring freshet is displayed in Fig. 2.12. The transport during the spring freshet spring tide on June 4th is strongly seaward (Fig. 2.12a) throughout the water column, with strongest transport at Red26. Transport on July 20th (Fig. 2.12b), ~30 days after the spring freshet ended, continues to be strongly seaward at Red26, but strongly landward at Am012. The landward flows at Am012 suggest possible release from peripheral bays and recirculation

from the South channel to the North channel. These transport plots provide information on ETM dynamics and support Hypothesis 1 and Hypothesis 2, SPM supplied during a freshet period is exported from the system primarily by strong tides and peripheral bays serve as important reservoirs.

The distribution of SPM between the individual W_s-classes also provides information on ETM dynamics. Fig. 2.9 shows the inverse analysis results for the North channel station, Am012. All W_s-classes demonstrate neap-spring fluctuations and seasonal fluctuations in concentrations. The smaller settling velocity classes (particularly C_2) show substantial concentrations at the surface, especially during and after the spring freshet (up to d 170). There is also a shift in the composition of the coarser material from C_3 during the freshet to C_4 after the freshet. This shift is not related to sand concentrations and may indicate the formation of larger aggregates after the spring freshet. Whether this shift is related to biological activity or a change in the character of the sediment supplied is unclear.

The smallest W_s-class (C_1, 0.014 mm s^{-1}) is essentially washload in the channel environments represented by all the ADP stations. It is not washload in peripheral environments however (Sherwood and Creager, 1990). Interestingly, C_1 concentrations are similar throughout the record for all stations, except that they are rather low at Red26 during and after the spring freshet. The higher washload concentrations at Am169, Tansy, and Am012 may indicate the influence of peripheral bays, primarily Youngs Bay and Grays Bay. Substantial neap-spring variations of C_1 at all stations also suggest that this material is being stored somewhere in the estuary on neap tides.

Storage of SPM is vital to secondary productivity in the system, because zooplankton populations are small during very high flow periods despite the presence of a large quantity of organic detritus and microbial productivity. Possibly, large numbers of zooplankters are exported along with the SPM on high-flow spring tides. In any event, storage of detritus in the system allows it to be incorporated into the food chain after the freshet. Another indication that material is being trapped on a time scale greater than one

neap-spring cycle is the fact that high concentrations of all W_s-classes continue beyond the freshet for at least one month (two months at Am012).

We quantify the retention of SPM by the system and consider H2, peripheral bays serve as important reservoirs for storage of SPM, using the residence time index, R_T (Fig. 2.13). Unlike salt (a conservative scalar), SPM settles. Only the maximum R_T (which is seen during spring tides) is meaningful – during most of the tidal month, much of the inventory of sediment is stored on the bed or in peripheral bays. The total R_T (for the North and South Channels together) suggests that sediment storage is small (less than 14 d) during the spring freshet. SPM is brought into the estuary and exported at the latest on the next spring tide. The situation is quite different after the freshet; SPM is stored in the system for more than a tidal month. Maximum R_T values are, in fact, of the same order as the time since the freshet, suggesting that material from the freshet is retained in the system on seasonal time scales. Given that there is essentially no storage of fine sediments on the bed during spring tides, it is likely that material is stored in peripheral bays. Mid-estuary sand flats are another possible storage site, but their ability to store fines is limited because they are wave-swept during most seasons. This is reflected in the high sand content of their bed material.

A question we cannot address directly here is the rate and timing of export from peripheral bays to the ETM. The maximum inventory of SPM in the ETM (the maximum value of the numerator of R_T) is ~1.5 kg m^{-2}, sufficient to create, upon deposition, a layer only 5 to 10 mm thick. This is consistent with the fact that sands are always dominant in grab samples. Still, thin layers of surficial fines are sometimes captured. We cannot rigorously distinguish, therefore, between continuous supply from the flats and episodic supply during storms and spring tides. But supply to the channel during periods of strong bed stress (storms and spring tides) seems likely.

Rouse number, P, is an important trapping parameter. Jay et al (2000) has hypothesized that intermediate values are most effective at trapping SPM in an ETM. Material that settles too slowly is washload. Material that settles too rapidly remains

SPM advection, judging by *A*, is more important on flood than ebb, which supports H3. Bedstresses are strong enough to erode flocs for only 1-2 hr on flood, and most flood peaks in *A* occur well after peak flood velocities. These factors also suggest that flood SPM peaks are largely advective. If, however, one judges the importance of advection by the presence of large W_s-class material that cannot be supported by immediate local erosion, then both ebb and flood SPM maxima could be advective in character. That is, ebb SPM peaks also tend to occur after the peak bedstress. Still ebb stresses are strong enough to erode flocs for a period of 3-6 hr and if there are any settling lags in the system, then ebb peaks may be largely local.

Fig. 2.16 shows the same properties as Fig. 2.15, but for a neap tide 20 days earlier in the freshet season. Neap tide *A* peaks are higher, consistent with H4 (advection is more important for sediment transport on neap tides than spring tides). Again, Tansy is in mid-ETM, and sand transport is negligible. In this case, the diurnal inequality is weak, but there is a small difference between the floods. Maximum total SPM and C_4 concentrations are similar to those on the springs, but mean SPM levels are lower. In particular, C_4 levels are quite low for much of the tidal cycle. The largest SPM peaks occur on flood, reflecting the fact that net SPM export is small. As with the spring tide, there is a tendency towards double ebb SPM maxima, possibly reflecting SPM input from Youngs Bay. Flood SPM maxima occur very early on flood during a period of weak shear, consistent with ETM occurring as part of a salt wedge advance. The first ebb SPM event of each pair tends to occur near peak ebb, while the second occurs during a period of high shear as salt is washed out. The relative magnitude of the paired peaks is inconsistent, and significant peaks do not occur on all ebbs.

The importance of advection, as indicated by *A* is somewhat more apparent during the neaps (Fig 2.16) than during spring tides (Fig 2.15), as flood peak SPM concentrations are much greater than ebb peaks and can only be explained by advection. Maximum ebb SPM levels are relatively small and do not show a consistent timing. The first of each doublet ebb SPM peak in C_4 appears to be explainable by local erosion,

whereas the second occurs as salt is washed out. The latter peak of each pair may then be advective.

In summary, examination of detailed time series of SPM processes support H3- advection is usually stronger on flood than on ebb. Still, the importance and timing of advection depends on position relative to the ETM. Ebb advection over the top of a retreating salt wedge is sometimes seen.

2.5.3 Trapping Efficiency and the Importance of Advection

Hypothesis H4 addresses tidal monthly variations in advection, as represented by low passed (subtidal) A. We suggest that advection should be more important under the stratified conditions associated with neap tides, because vessel observations regularly show mid-depth SPM maxima associated with the velocity maximum at the top of the intruding salt wedge. Evidently, high bedstresses near the mouth of the estuary are more capable of suspending material than is the case in the ETM itself. Consistent with H4, tidally-averaged values of A are almost always greater on neap than on spring tides at all the stations (Fig. 2.17a). Spring-neap differences in A are greatest at Red26 during the high-flow season, when stratification is maximum. Finally, note that the spring-neap differences in A shown here are, in fact, conservative, because the bottom ADP bin is 2 to 3 meters off the bed. This effectively puts a floor on H_m at the level of the lowest bin and causes fluctuations below this level to be missed. During periods of strong bedstress when local erosion and deposition rather than advection are dominant, the SPM maximum is at the bed, and H_m should be less than the value calculated from the ADP data.

The relative values of A at the various moorings in the South Channel also provide information regarding ETM processes (Fig. 2.17a). Red26 has the highest advection numbers in the spring, corresponding with highly stratified conditions at this station. During this period, the mean ETM position is located near Tansy, and high A values at Red26 may correspond to advection of SPM from seaward of Red26 toward the

ETM. Am169 has higher advection numbers during summer and early fall, indicating an ETM in close proximity to this station, consistent with the discussion of Fig. 2.6. Tansy has highest *A* values in the late fall, which may correspond with a seaward movement of the ETM back toward Tansy.

Hypothesis H5 addresses the seasonal variations and spatial heterogeneity of trapping efficiency, as quantified by *E*. We show in Fig. 2.17b the *E* time series for the three stations most frequently in the center of the ETM: Am169, Am012 and Tansy. Our calculated E is based on SPM observed in the water column, at least 1.8 -2.7 m off the bed. Neap tides are characterized by low *E* values, because SPM is accumulated near the bed and in peripheral bays at this time. The high *E* values observed on spring tides reflect accumulation of sediment during the previous neap. *E* is clearly variable in space; the North channel station AM012 shows consistently the highest *E* values, despite the fact that SPM supply to the North Channel is rather indirect. It is evident in Fig. 2.18 that all three stations show an inverse relationship between *E* and river flow Q_R. *E* is maximal during low flow periods and exhibits spatial heterogeneity, consistent with H5. Conclusions about *E* are indirect, however, because of lags built into system. *E* was maximal as the flow fell after the freshet, in part due to of storage of SPM in peripheral bays. We cannot directly answer questions regarding the efficiency of the trapping processes in the ETM itself.

2.6 Conclusions

We examined ETM dynamics of the Columbia River estuary over a range of time scales utilizing moored acoustic and vessel data. Results support H1: SPM is exported from the Columbia River estuary primarily on spring tides during and shortly after the spring freshet, as evidenced in the total transport and SPM time history results for each station. The evidence also supports H4. Elevated values of *A* indicate that advection is more important on neap tides than spring tides. Also, predictions of sand and floc at the bottom bin coupled with efficiency, advection, inverse analysis results, and shear

parameters suggest the importance of advection in the mid-ETM on neap tides. Flood ETM events were found to be more advective than ebb events, especially on neap tides during the spring freshet supporting H3. E time series and scatter plots suggest the most effective trapping occurs during neap tides with low river flow, supporting H5. Particle trapping was also more effective in the North channel, despite its indirect SPM supply. The high sediment concentrations after the spring freshet and R_T plots provide evidence for storage of SPM in peripheral bays on both tidal monthly and seasonal scales (H2). The importance of SPM storage in peripheral bays renders results regarding H5 somewhat ambiguous. High E values during the high-flow season may be more related to storage in peripheral areas than variations in channel flow processes. A longer record is needed to resolve this question. Finally values of low passed, tidal maximum Rouse number for large aggregates were typically between 2 and 3 during periods of SPM retention, and 1 to 2 during periods of export. This is consistent with the idea that only material within a farily narrow range of P values can be efficiently trapped in an ETM.

Moored instrument time series of E, P_4, A, and R_T, total SPM concentration, W_s-class specific SPM concentrations, and velocities were useful in combination as indicators of the movement and location of the ETM. Determination of W_s-class concentrations via inverse analysis proved to be a powerful tool for studying suspended particulate dynamics in the Columbia River estuary. Gravimetric samples, W_s data, and other vessel observations were vital for the calibration and interpretation of the inverse analysis calculations. Thus, both vessel and moored instrument data are needed to understand ETM processes in intra-tidal to seasonal time scales. The joint use of moored acoustic and cruise data provides unprecedented and significant temporal and spatial resolution of sediment dynamics. This approach to estuarine sediment dynamics should have broad utility beyond the system considered here. These and similar studies can be applied to the realm of science and policy issues related to dredging, dredged material disposal, pollutant dispersion, and estuarine management.

2.7 Symbols

A	advection number
C_i	volume sediment concentration of the i^{th} settling velocity
C_i	volume total sediment concentration of the i^{th} settling velocity
C_{1i}	volume sediment concentration at the first bin
C_d	drag coefficient
C_m	maximum concentration of sediment
C_s	source concentration of sediment
D	elliptical nominal diameter
E	Trapping Efficiency
K_s	eddy diffusivity
H	height scalar
H_m	height of maximum sediment concentration
L_s	sediment excursion
P	Rouse paramter
R_T	Residence Time index
U	along-channel velocity
$<U>$	mean along-channel velocity
U_*	shear velocity
U_{*sf}	skin friction velocity
U_T	tidal velocity scale
W_s	Settling velocity
i, i	W_s class indicator
j	bin number
k	Von Karman's constant, equal to 0.408 (Nowell, 1983)
m	number of Ws classes
n	number of depth bins for analysis
t	time

u	vertical velocity
v	vertical velocity
w	horizontal velocity
ω	semidiurnal frequency scalar
x	vertical coordinate
y	vertical coordinate
z	horizontal coordinate
z_1	height of the first ADP bin
z_a	height of the bedload layer
α	one way sound absorption
γ_0	coefficient of proportionality (empirical resuspension parameter)
ΔU	surface along-channel velocity minus bottom along channel velocity
ϵ_a	sediment concentration at the height of the bedload, z_a
ϵ_b	volume concentration in bed, 0.65 (assuming a porosity of 0.35)
π	acceleration term in non-dimensional transport equation
σ	non-dimensional distance from bed
τ_b	bed shear stress
τ_c	critical shear stress

2.8 Acknowledgments

This work was funded by the Office of Naval Research AASERT grant, N00014-96-1-0893, and the National Science Foundation Grant *Columbia River Land-Margin Ecosystem Research Project*, OCE-9412928, and SGER, *Amplification of El Niño-Southern Oscillation (ENSO) Climate Effects in Estuaries*, OCE-9816083.

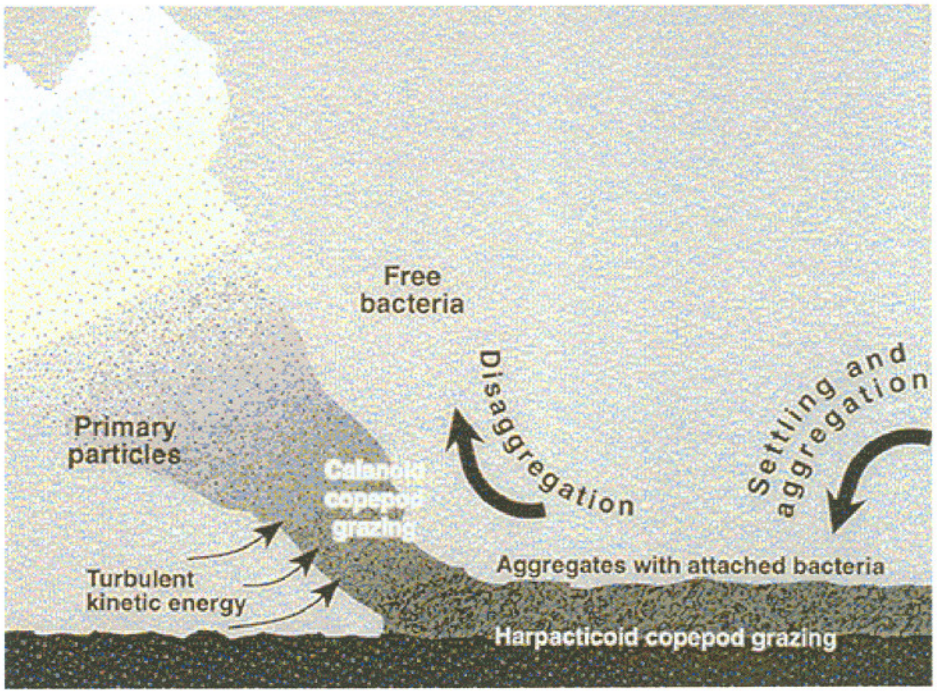

Figure 2.1. Estuarine Turbidity Maximum "event" depicting interaction between biological, chemical, geological, and physical processes (CRETM-LMER, 2000).

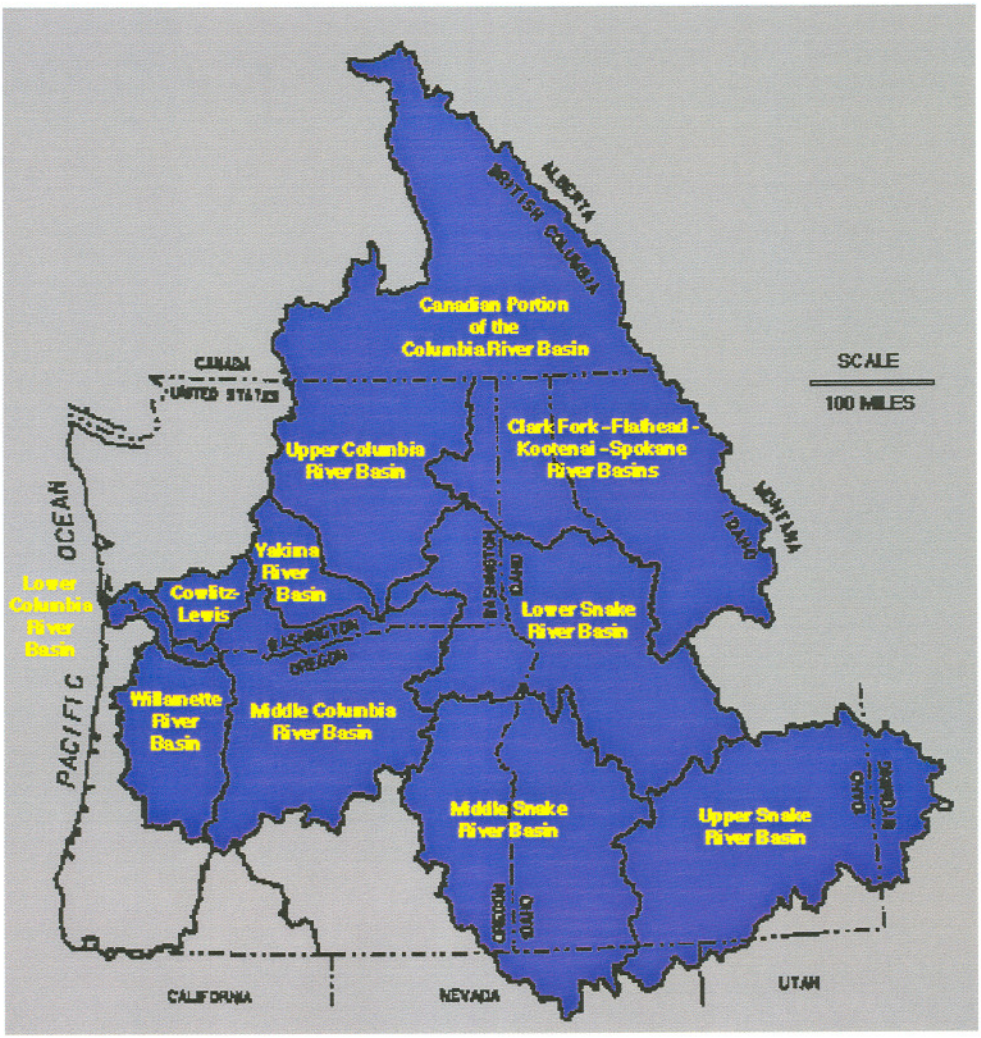

Figure 2.2. The drainage basin of the Columbia River. The Columbia River has a drainage basin area of 660,500 km^2 and an annual average riverflow of approximately 7,500 m^3 s^{-1} (USACE, 1999).

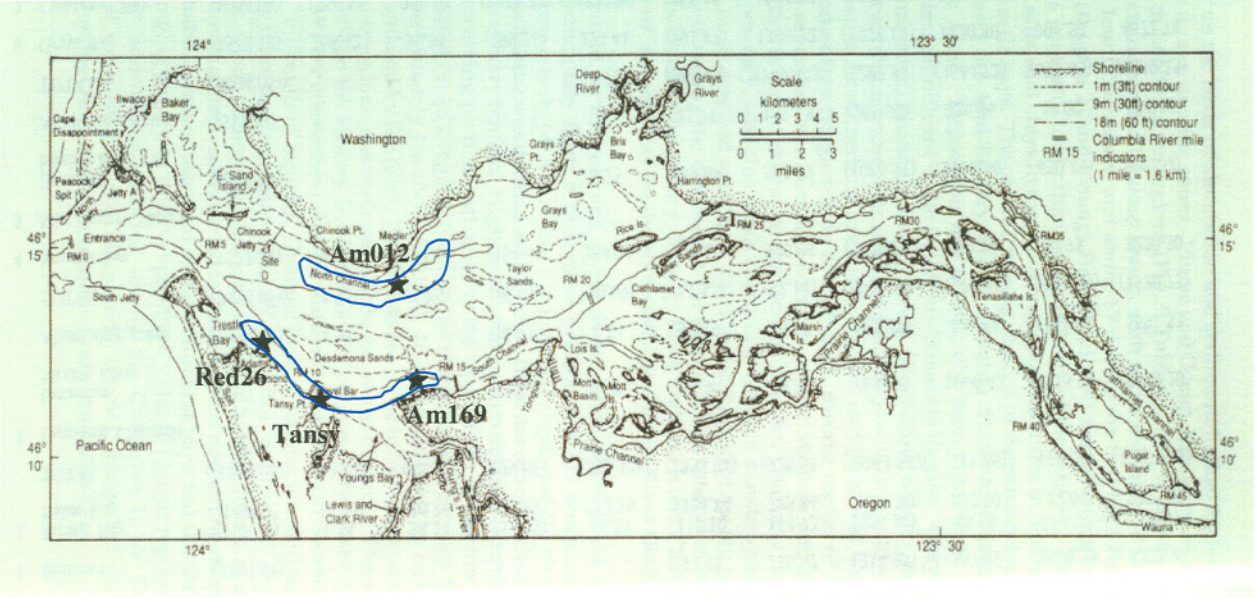

Figure 2.3. Map of Sontek moored Columbia River Estuary Observation and Forecast System (CORIE) ADP stations (★) in the Columbia River Estuary for 1997. Red26 and Am169 had 0.5 MHz ADPs, while Tansy and Am012 had 1.5 MHz ADPs (modified from Simenstad et al., 1990). South and North channel ETMs are depicted by blue outline.

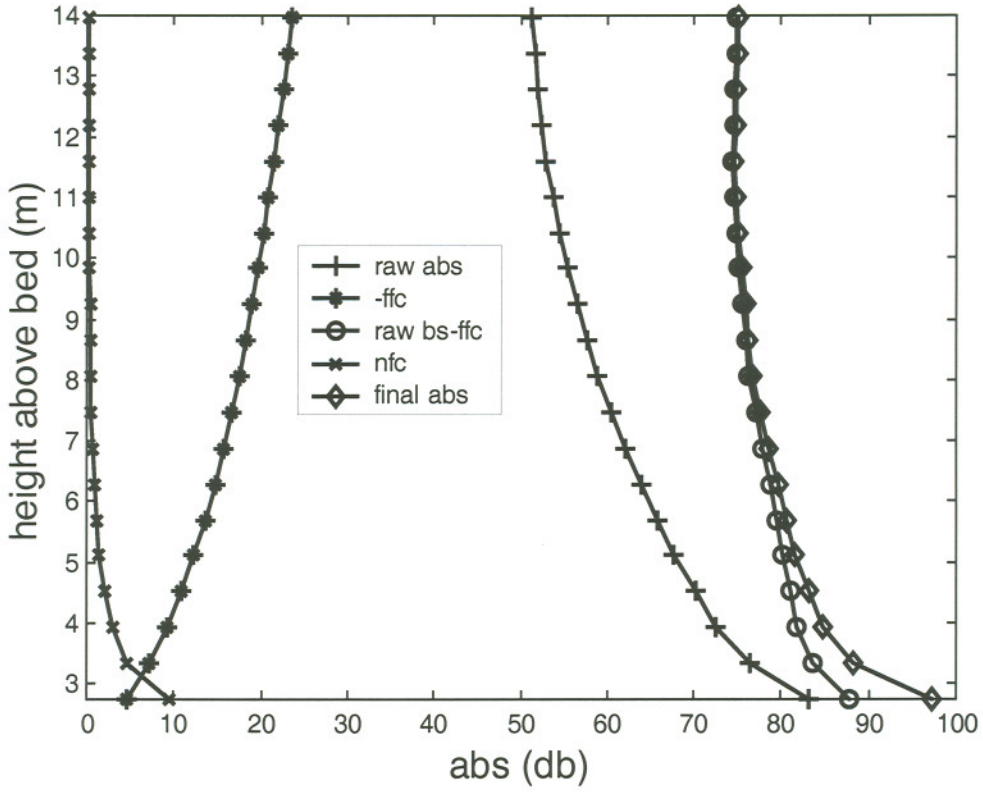

Figure 2.4. Backscatter corrections at Red26. Nearfield corrections (nfc), and farfield (ffc) corrections were applied to the acoustic backscatter (abs) before it was converted to sediment concentrations.

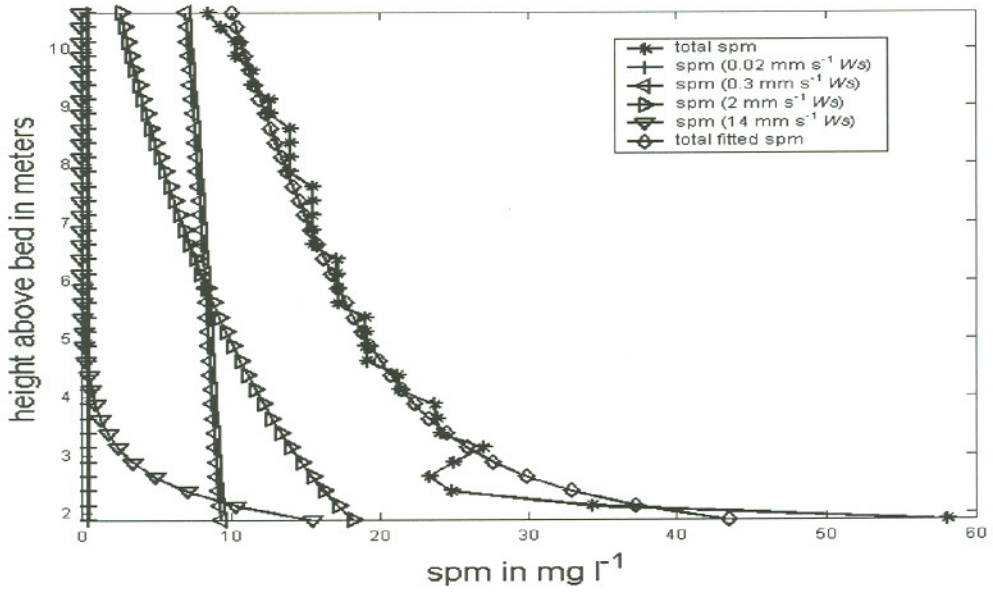

a)

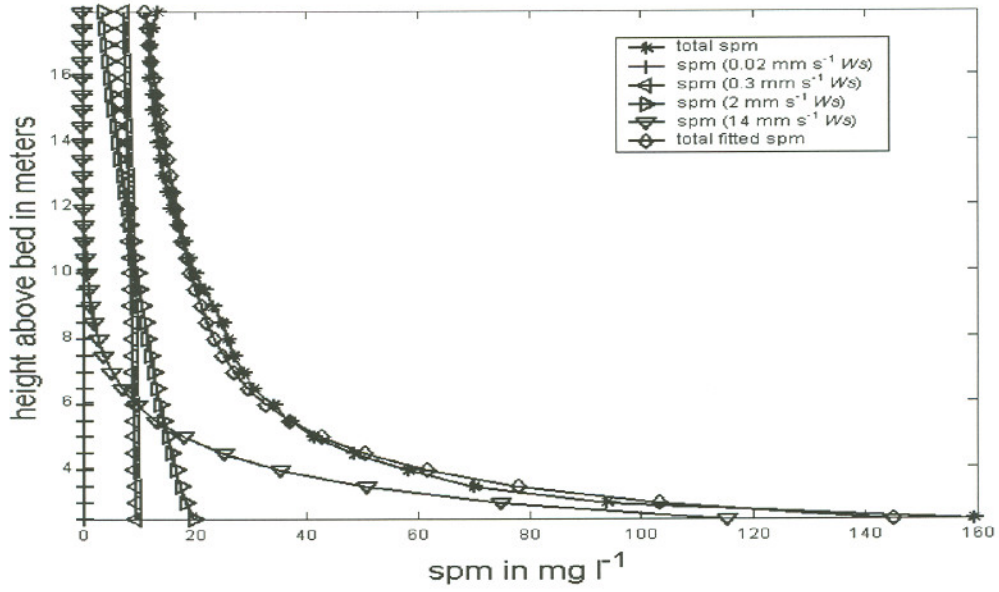

b)

Figure 2.5. Examples of inverse analysis fit: using four settling classes at Tansy (1.5 MHz-a) and Am169 (0.5 MHz-b). The results in (a) suggest that the nearfield corrections recommended by the manufacurers may need improvement.

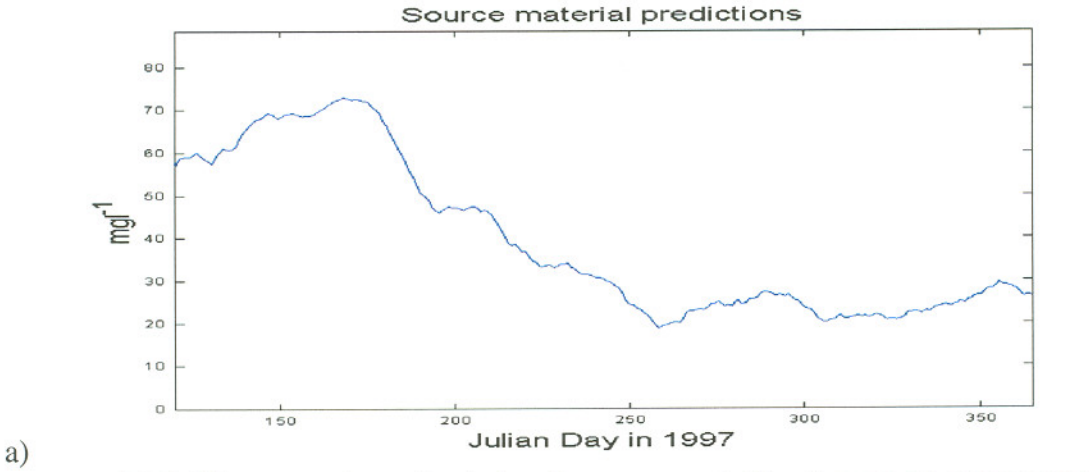

a)

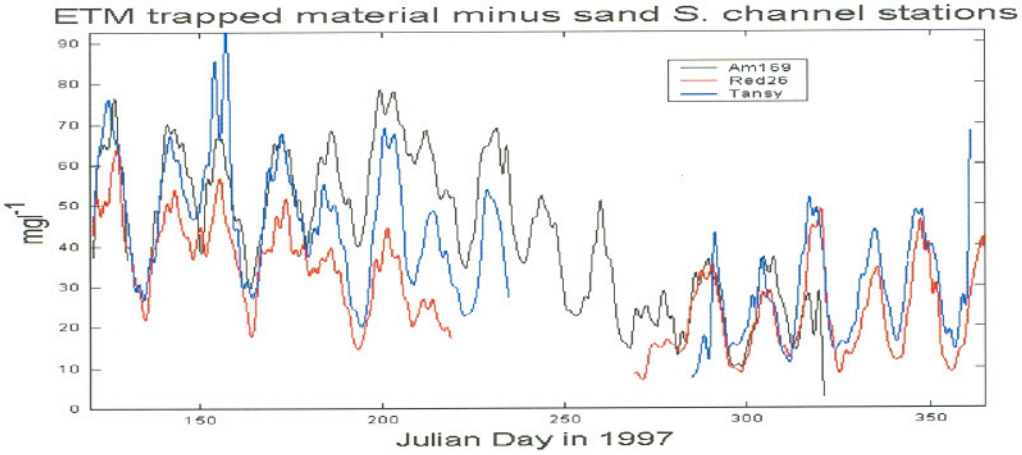

b)

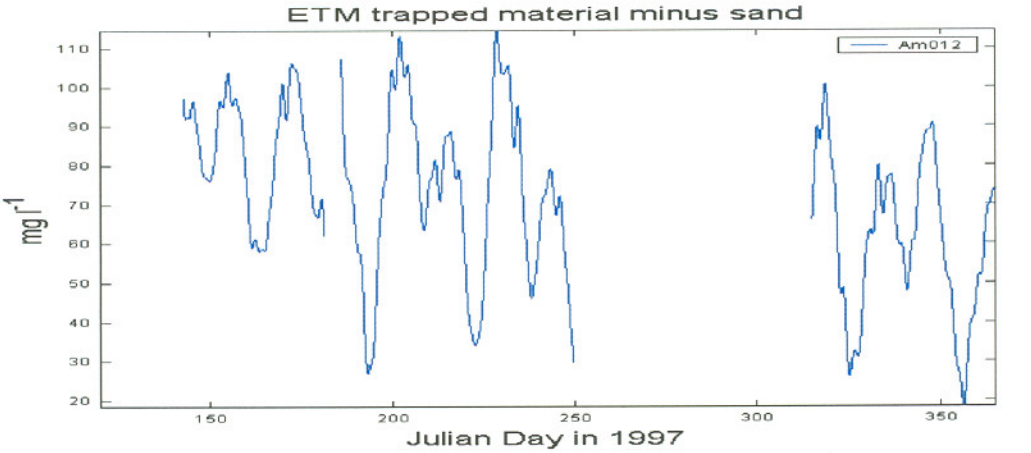

c)

Figure 2.6. Estimated fluvial source material (a) low pass filtered estimated fluvial sediment supply minus estimated sand), and low pass filtered trapped in the ETM at all stations, (b) and (c). ETM trapped material consists of three W_s classes (0.3 mm s^{-1}, 2.0 mm s^{-1}, and 14.0 mm s^{-1}) minus predicted sand concentrations. Gaps in the SPM record between ~d. 230 and 315 indicate biofouling of a duration that varied between stations.

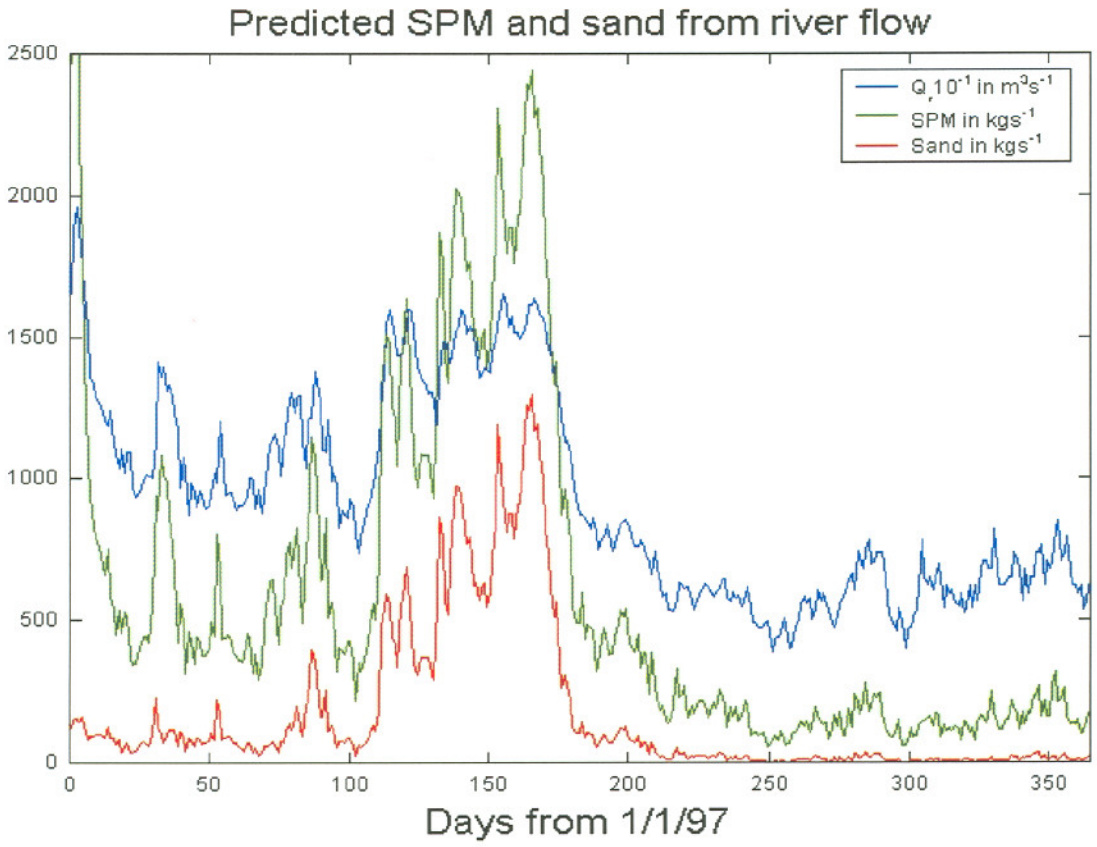

Figure 2.7. River flow (Q_r) at Beaver army terminal, River Mile (RM) 53 during 1997, estimated total fluvial sediment load, and estimated fluvial sand supply. The total load predictions are the sum of predictions for Columbia River at Vancouver, Washington and the Willamette at Portland, Oregon. The sand transport estimate is for the Columbia at Vancouver only. The sand supply for early January is greatly underestimated, because most of the flow at the time was from the Willamette and other Lower Columbia river tributaries.

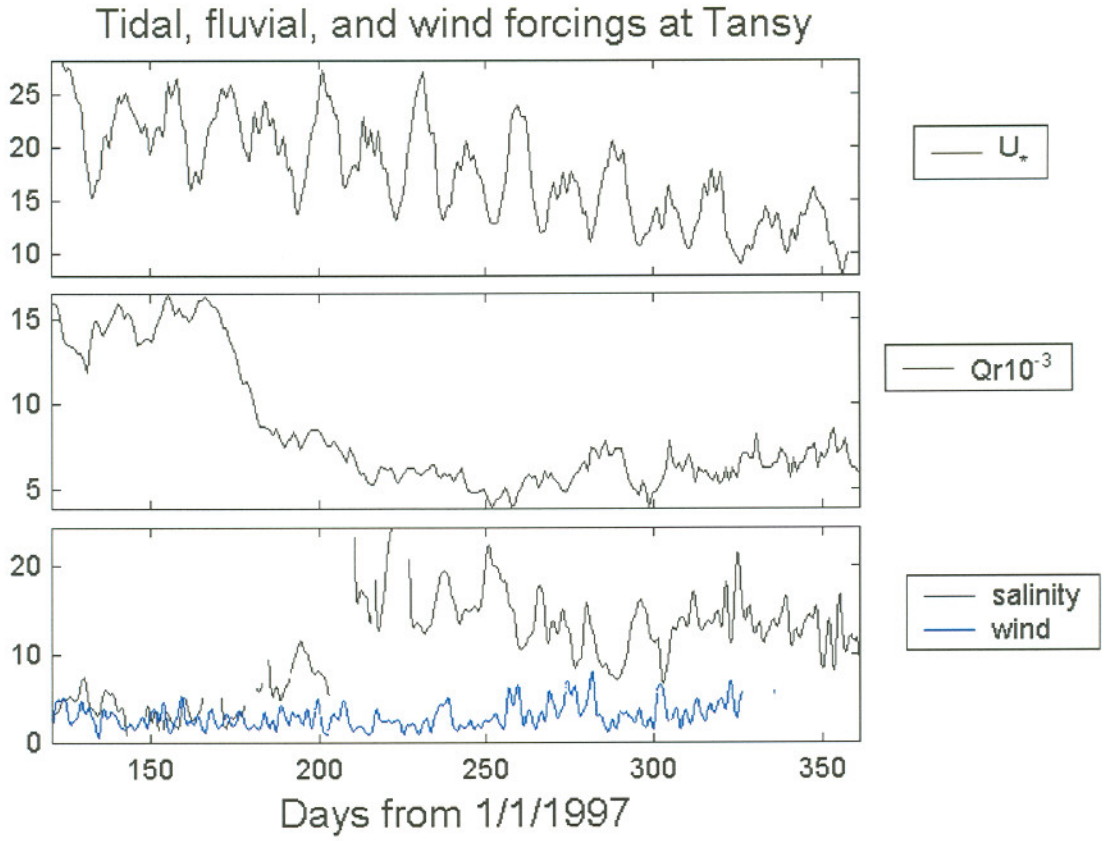

Figure 2.8. Tidal, fluvial and low passed wind forcing at Tansy. Shear velocity, U_*, is in mm s^{-1}, riverflow, Q_r, is in thousands of m^3 s^{-1}, and wind from the Columbia Bar is given in m s^{-1}

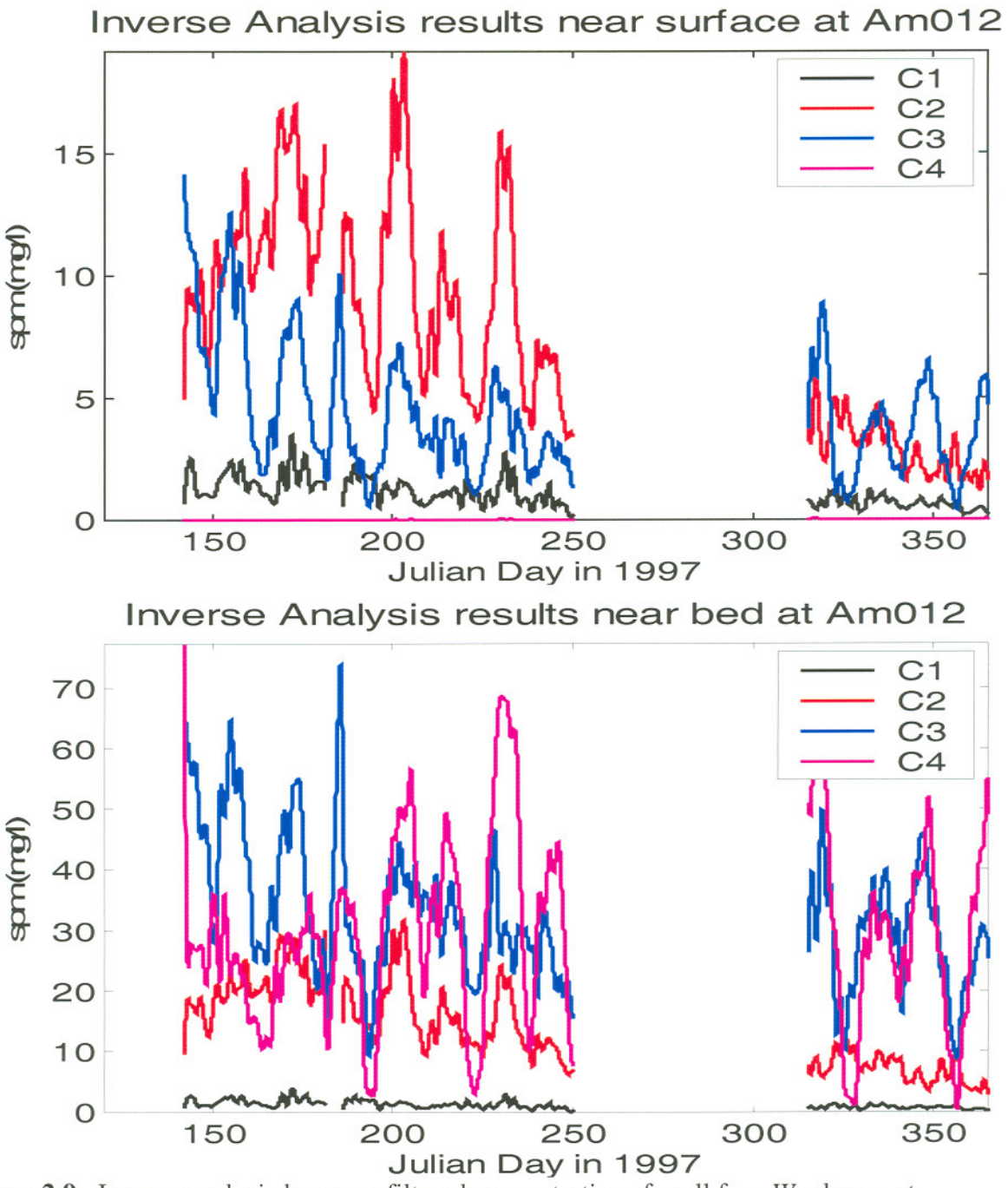

Figure 2.9. Inverse analysis low pass filtered concentrations for all four W_s-classes at Am012, near the surface and bed. Neap-spring fluctuations are evident in all settling classes, as well as seasonal variations.

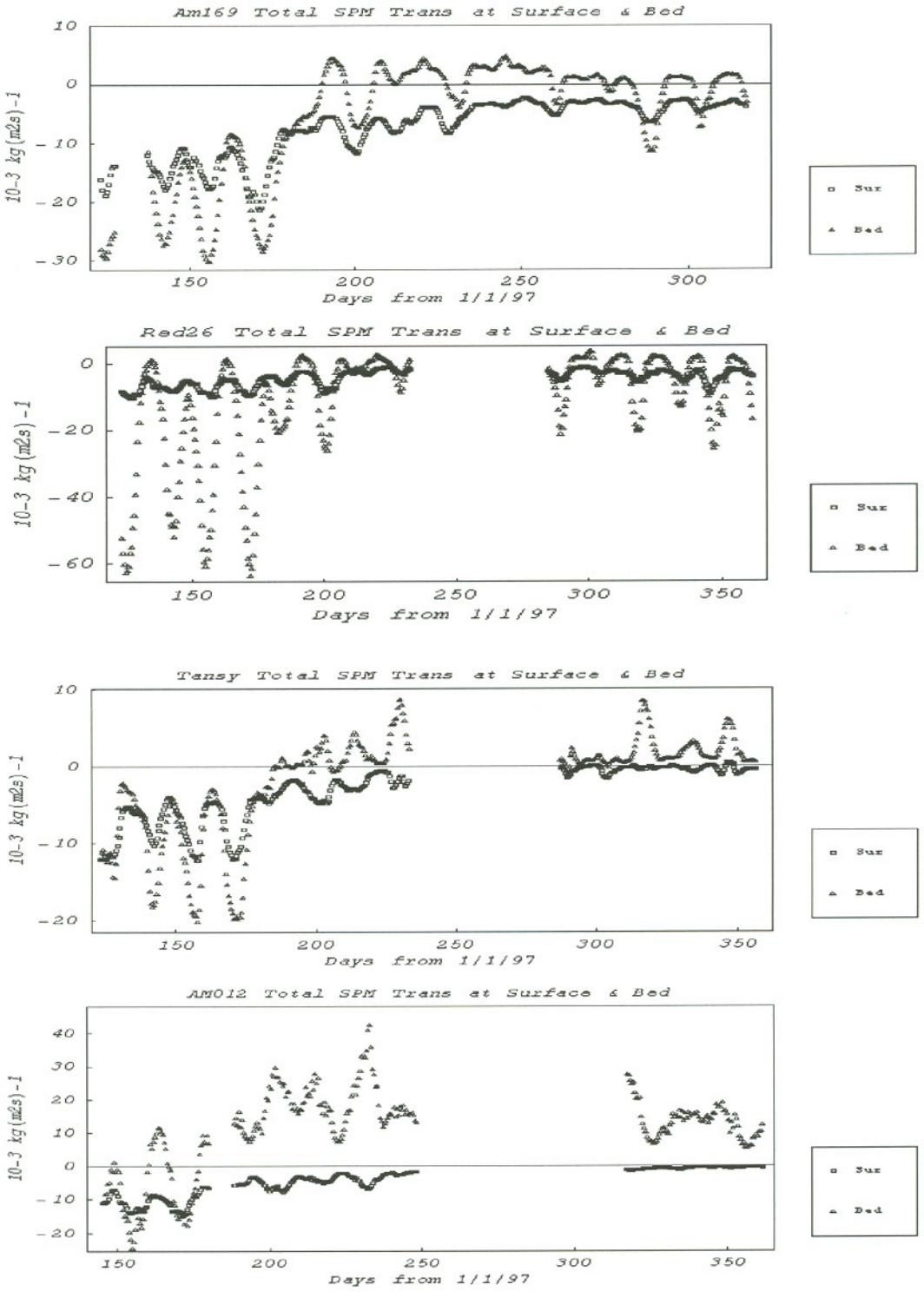

Figure 2.10. Total net SPM transports at all CORIE stations for 1997, near-surface (©) and near-bed (∫). Negative velocities are seaward.

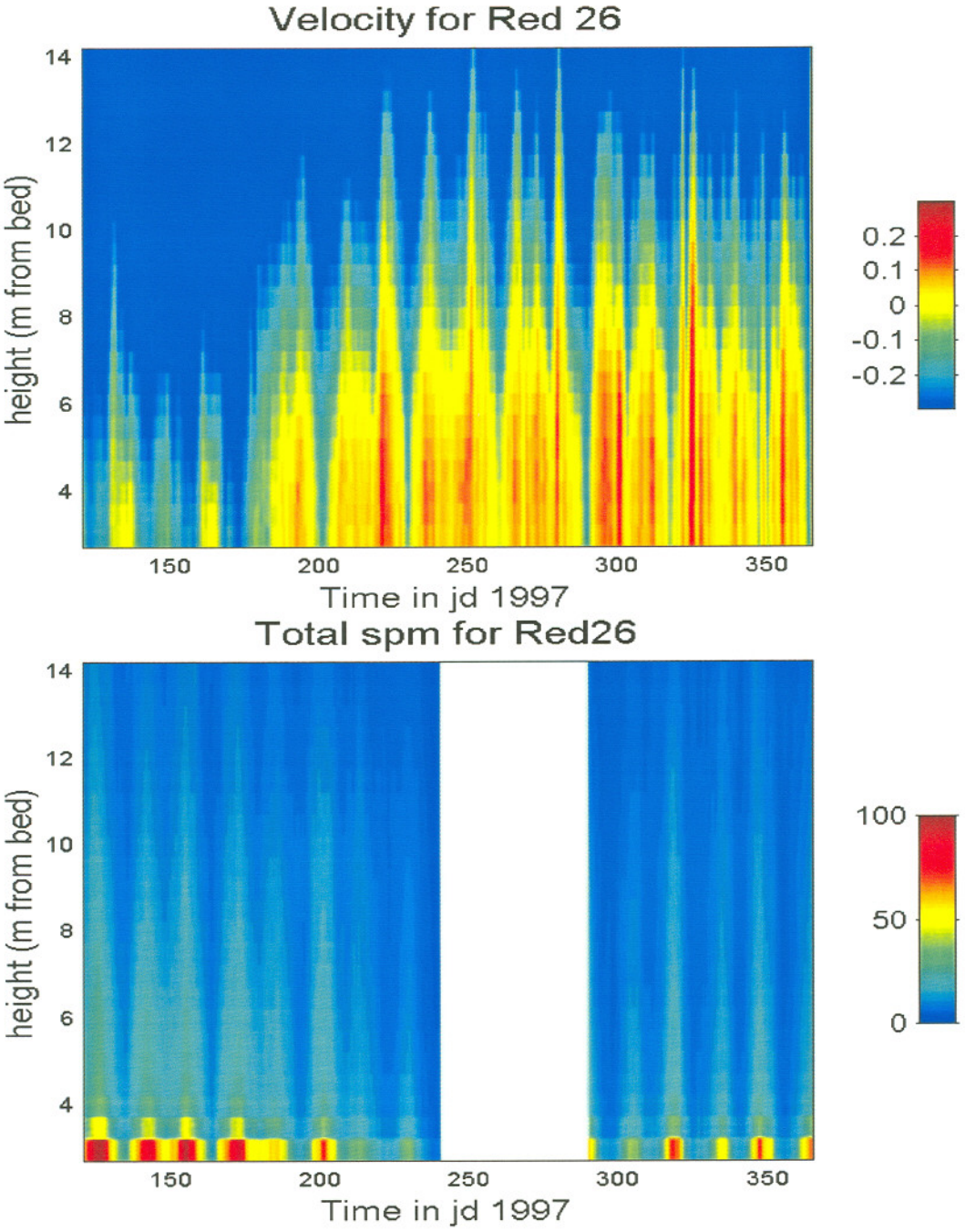

Figure 2.11. Along-channel velocity (m s^{-1}) and total SPM (mg l^{-1}) at Red26 from May to December 1997. Both have been low pass filtered. Negative velocities are seaward.

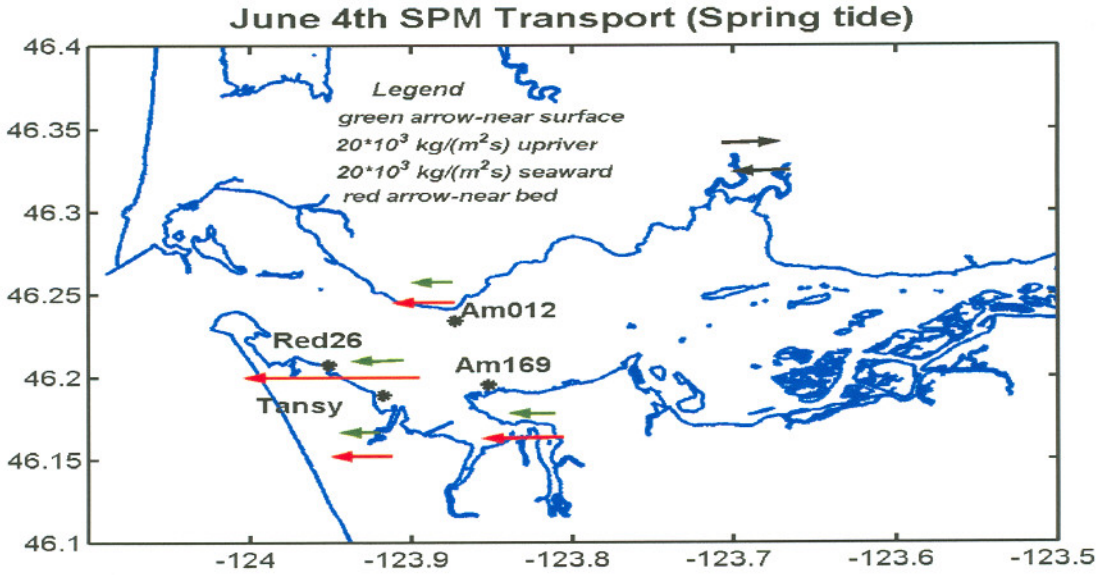

a)

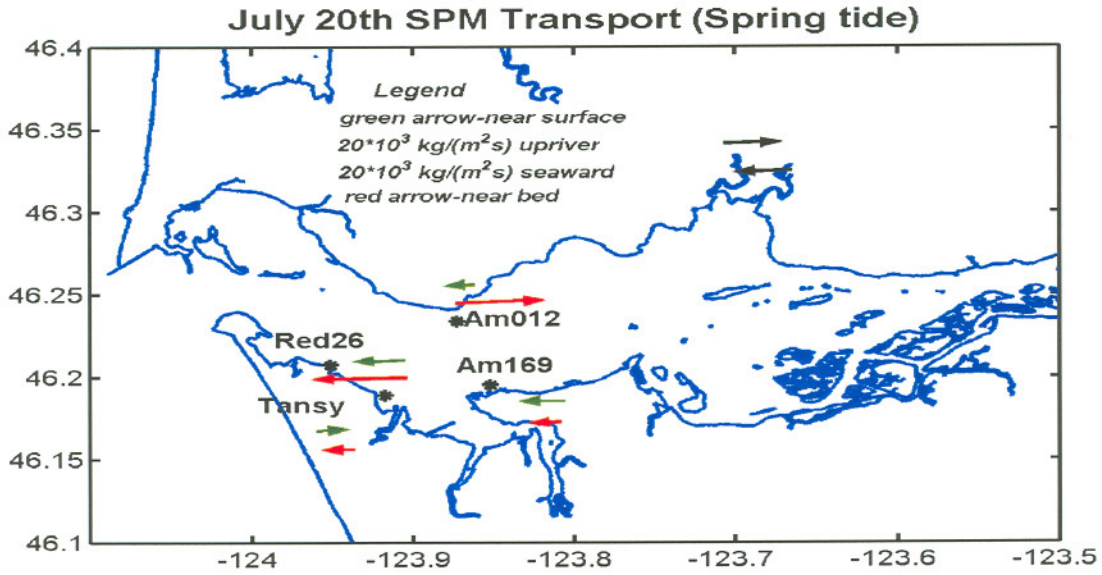

b)

Figure 2.12. June 4th spring tide SPM transport (a) and July 20th spring tide SPM transport (b) at CORIE ADP stations. The green arrows refer to transport near the water surface and red arrows refer to transport near the bed. Arrows pointing to the right refer to upriver transport and to the right refer to seaward transport. June 4th was during the spring freshet and July 20th was about 30 days after the freshet ended.

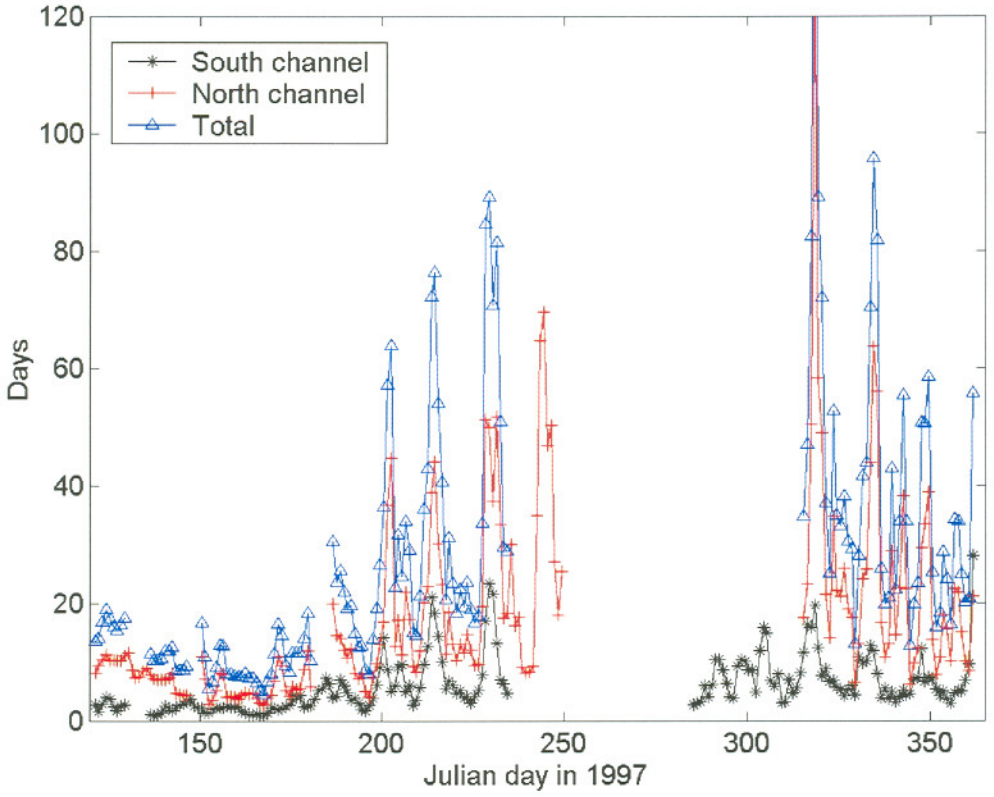

Figure 2.13. SPM residence time index in the Columbia River Estuary for the South channel ETM (*), North channel ETM (+), and for the two in combination (Δ). Residence time index was not determined for periods where biofouling was present.

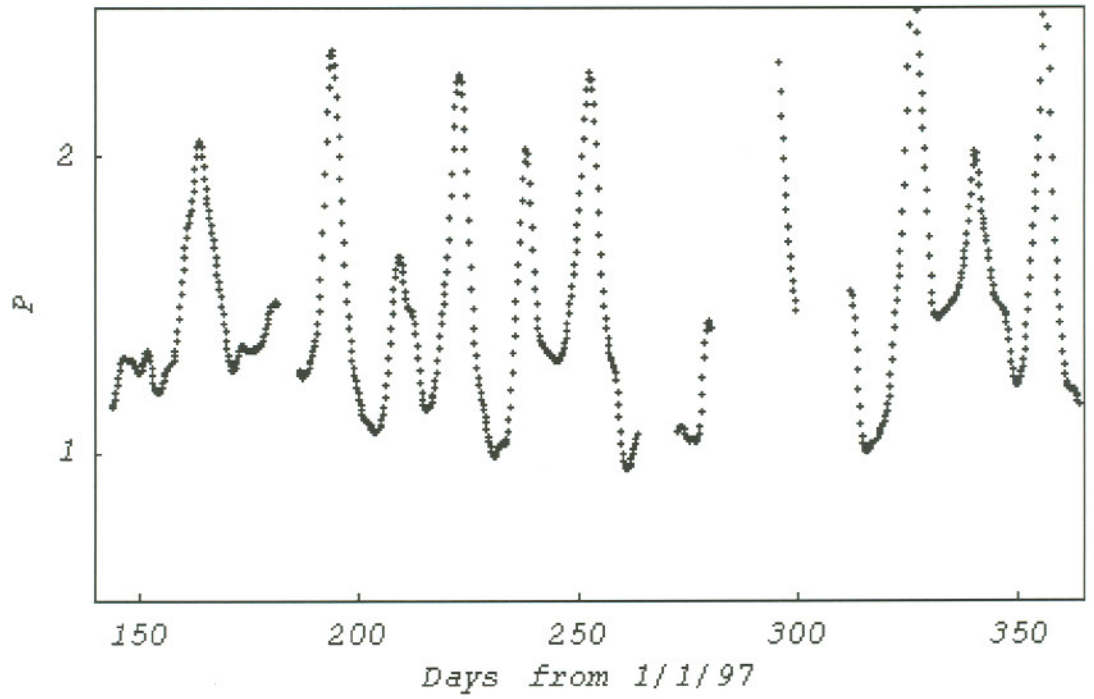

a)

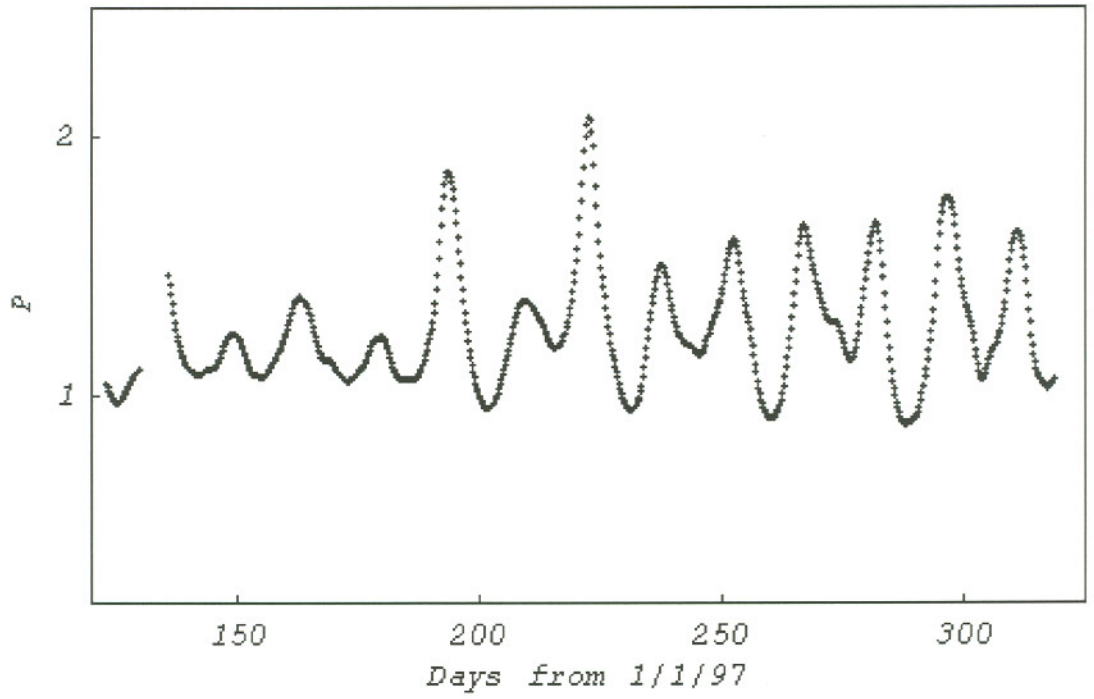

b)

Figure 2.14. Low pass filtered large aggregate Rouse number, *P*, for Am012 (a) and Am169 (b).

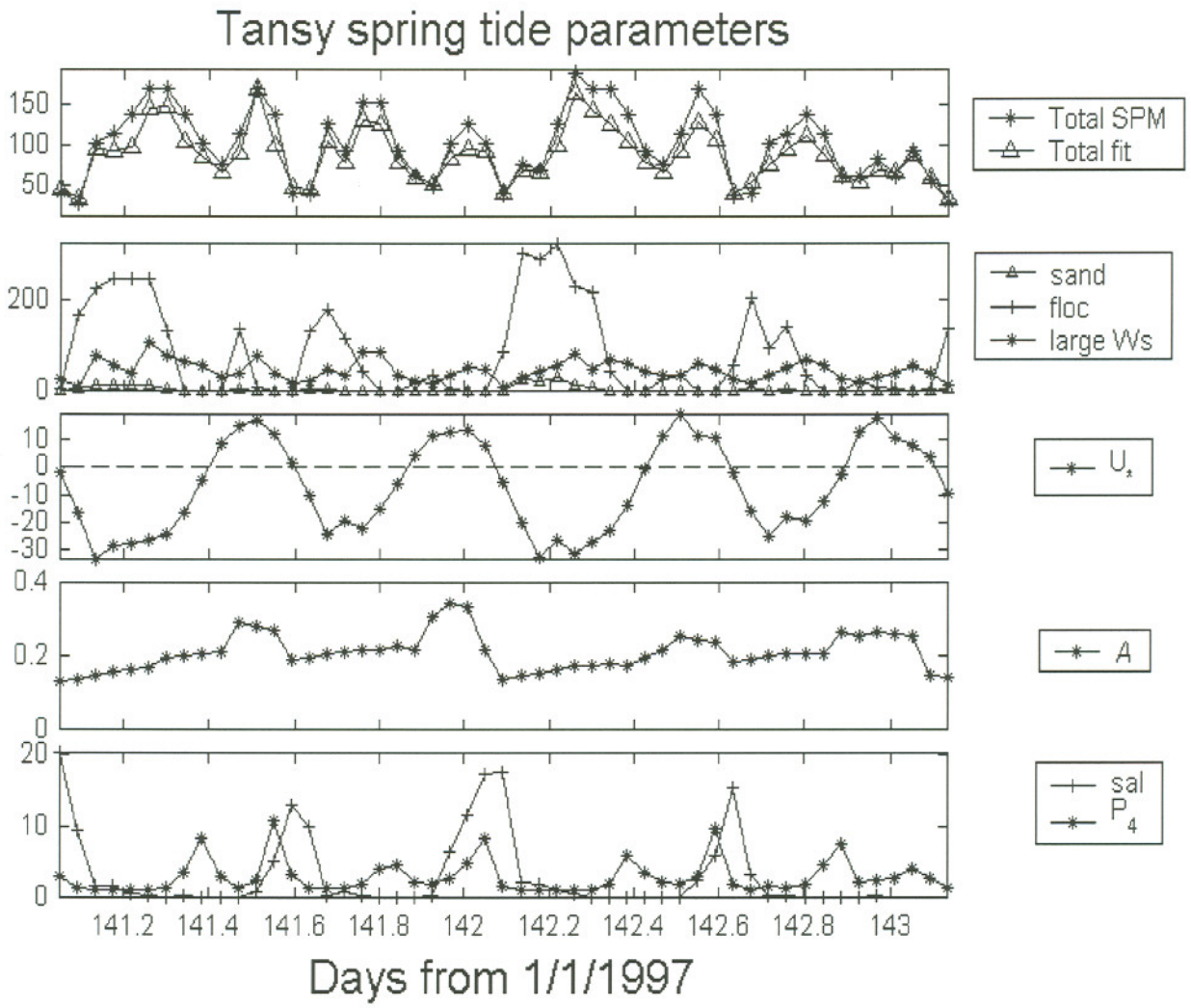

Figure 2.15. Total SPM (*) and total fitted SPM from the inverse analysis (2 m off the bed). Sand and floc predictions and large W_s (*), C_4 from the inverse analysis. Shear velocity, U_* (*), in mm s^{-1}, advection number, *A* (*), salinity, and Rouse parameter, P_4 (*), during a 2 day spring high flow spring-tide period at Tansy.

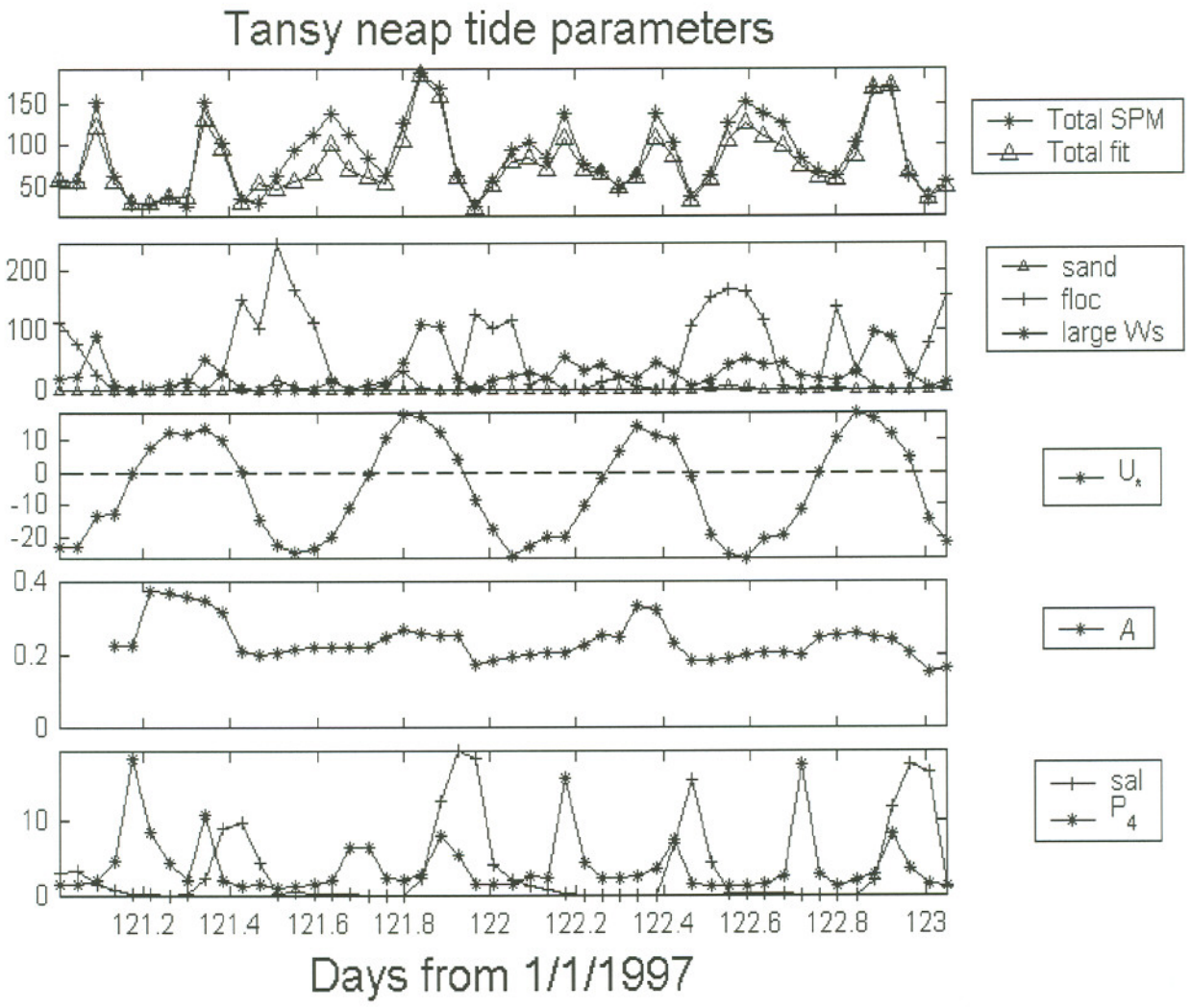

Figure 2.16. Total SPM (*) and total fitted SPM from the inverse analysis (2 m off the bed). Sand and floc predictions and large W_s (*), C_4 from the inverse analysis. Shear velocity, U_* (*), in mm s^{-1}, advection number, *A* (*), salinity, and Rouse parameter, P_4 (*), during a 2 day spring high flow neap-tide period at Tansy.

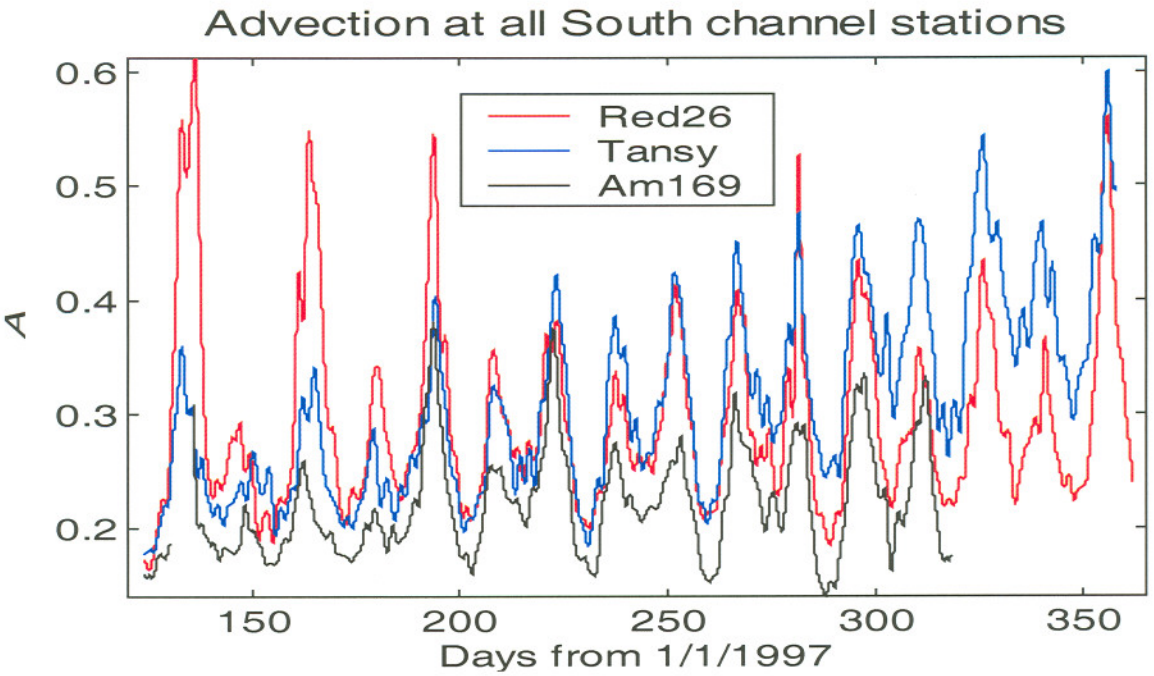

a)

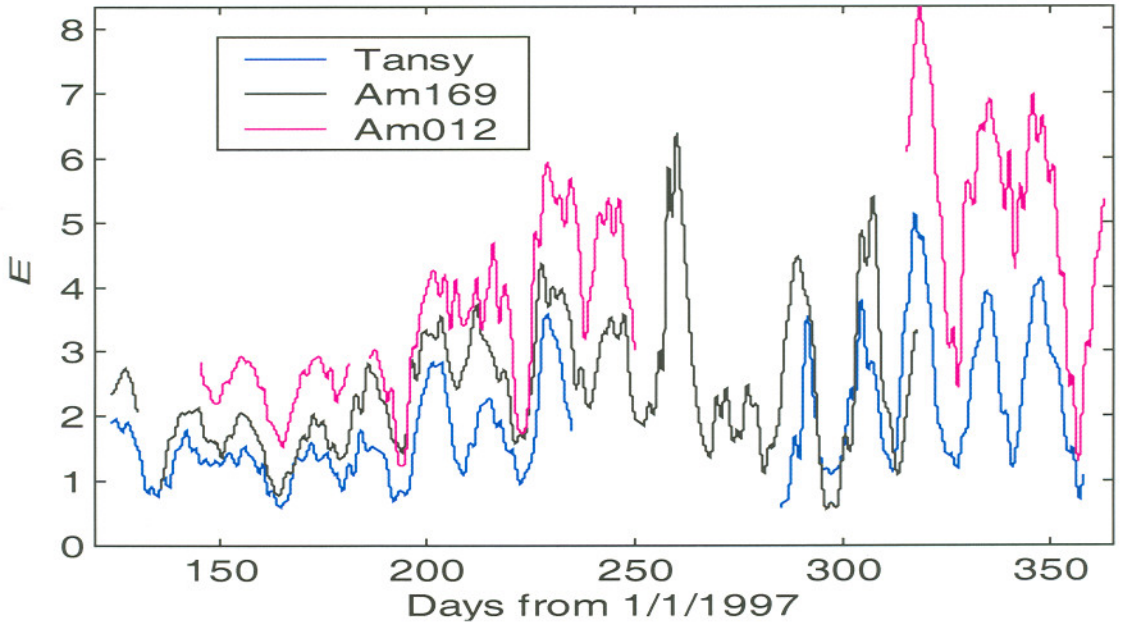

b)

Figure 2.17. Low-pass filtered *A* for all South channel stations (a) and low pass filtered trapping efficiency (*E*) for Am169, Am012 and Tansy (b).

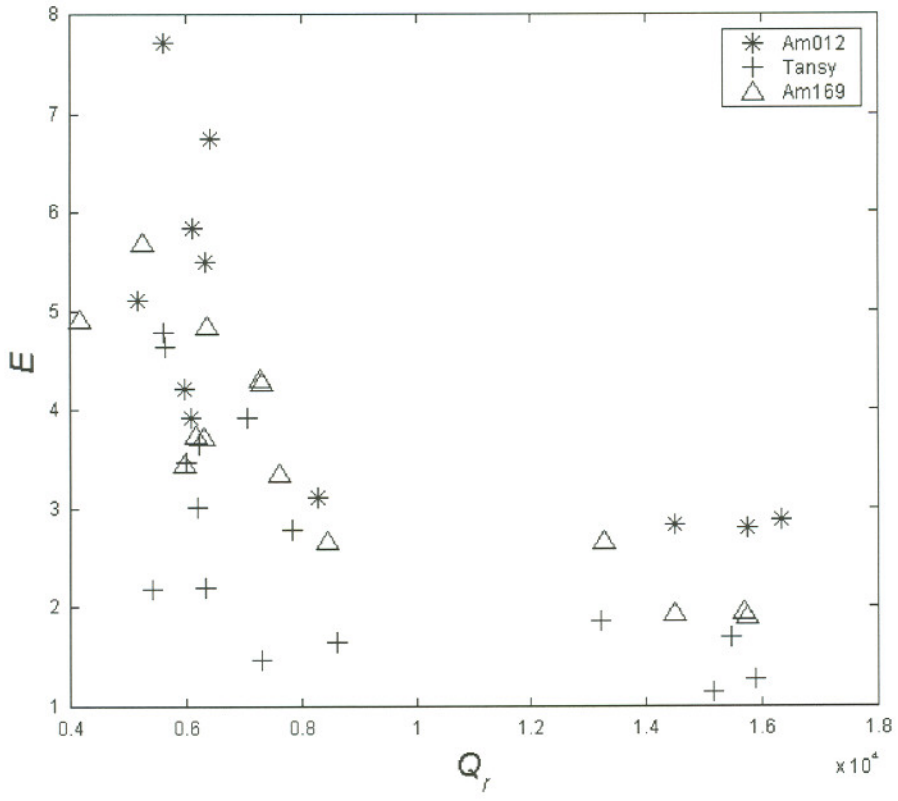

Figure 2.18. Riverflow (Q_r) in $m^3\ s^{-1}$ vs Trapping Efficiency (E) at Am012 (*), Tansy (+), and Am169(Δ).

Table 2.1. Station information from the four CORIE ADP stations during 1997.

Station information	**Red26**	**Tansy**	**AM169**	**AM012**
# of beam	3	4	3	4
Frequency (MHz)	0.5	1.5	0.5	1.5
Blanking distance (m)	1.0	0.25	1.0	0.25
Bin size (m)	0.50	0.25	0.50	0.25
suspect biofouling period (days from 1/1/97)	235-280	235-285	none	270-315
Mean temperature (°C)	13.24	13.61	15.06	13.77
Mean depth (m)	16.86	13.32	19.22	21.12
First bin depth (m)	2.72	1.87	2.72	1.87
Number of depth bins always covered by water (m)	24	36	29	67

Table 2.2. Large settling velocity class (14 mm s^{-1}): diameter (D), density (p_s), critical velocity (u_{*c}), critical shear stress (τ_c) for aggregates and sand. Floc diameter was determined by using formula by Sternberg et al., 1999.

D (m)	ρ_s (g cm^{-3})	u_{*c} (m s^{-1})	τ_c (dynes cm^{-2})
sand-$1.25*10^{-4}$	2.65	$1.01*10^{-2}$	1.01
aggregate-$1.40*10^{-3}$	1.02	$3.70*10^{-3}$	$1.37*10^{-1}$

CHAPTER 3

Methods for Determination of Sediment Concentration

The purpose of this chapter is to describe in detail procedures used to determine SPM concentrations from ABS and OBS. Both ABS and OBS sensors must be calibrated against SPM samples. In addition, ABS profiles must be corrected for absorption of water and sediment, beam spreading and near-field effects. The necessary sediment characterization data (consisting of gravimetric, OBS, and Owen Tube data) were obtained during LMER cruises. Dr. Fred Prahl of Oregon State University conducted gravimetric analyses of pumped SPM samples (Simenstad et al, 1994). An OBS was located on the pump platform, so these samples were used to provide a direct calibration of OBS. ABS was calibrated using OBS as an intermediary. Size spectra were determined from Owen Tube samples provided by Dr. Denise Reed as per Reed and Donovan (1994). Owen Tube results were analyzed in order to determine characteristic W_s-classes, of which four were identified. Subsequently, a modified inverse analysis method was applied to determine distinct W_s-class concentrations from total SPM concentrations.

3.1 Optical Backscatter Calibration

OBS data were employed as an intermediary in the calibration of moored ABS signal level to SPM concentration. The OBS sensors were calibrated in the laboratory at the beginning and end of the field season. SPM concentrations were determined from gravimetric analysis of pump samples taken at the same depth as OBS measurements.

The OBS vs. ABS calibration values varied with season, from a slope of 1.82 mg (l NTU)$^{-1}$ in May and October, to a slope of 2.13 mg (l NTU)$^{-1}$ in July (Table 3.1). The R^2 values varied from 0.86 in July, 0.88 in May, and 0.92 in October. During the seasonal cruises, OBS data were collected every 15 to 30 minutes, often in the vicinity of the moored ADPs. Therefore, we utilized the OBS-SPM calibration at times when one of the LMER research vessels collected samples within 50-100 m of the CORIE ADP moorings to develop a relationship between ABS and SPM.

3.2 Acoustic Backscatter to SPM

The correction and calibration of the ABS from each instrument is essential in providing meaningful SPM concentration information. Two frequencies of bottom moored, upward looking Sontek ADPs were used to obtain velocity and ABS signal level: 500 kHz (three-beam) instruments at Tansy and Am012, and 1.5 MHz (four-beam) instruments at Red26 and Am169 (Table 3.2).

There are several steps in the ABS vs. SPM calibration:

Pre-processing: pre-processing converts ABS data from counts to dB; the conversion is weakly dependent on instrument frequency.

Signal strength correction: the initial correction followed the signal strength correction for Sontek ADP's (Sontek, 1996; Sontek, 1997; Sontek, 1998). This accounted for beam spreading and water-column sound absorption that vary primarily with instrument frequency and slightly with salinity (Table 3.2). The correction for along-beam decay is:

$$SS = 20 \log R_b - 2\alpha(R_b) \qquad (3.1)$$

where signal strength SS is in dB, α is one way sound absorption (dB m^{-1}), R_b is along beam range in m (Sontek, 1996; Sontek, 1997). Note that α depends in general on

temperature, salinity and frequency, but the salinity dependence is weak at frequencies above 500 MHz. Beam spreading and along-beam decay are the largest corrections, but near-field corrections are also very important.

The near-field correction: Very close to the transducer head, an acoustic signal cannot be treated as coming from a simple source, and the actual diameter of the transducer must be taken into account. We applied the near-field correction to pressure used by Sontek (1998), as derived from basic acoustical principles (Clay and Medwin, 1977):

$$P_{near} = \left| \sin(k_w(r_0 - R_b)\exp[-ik_w(r_0 + R_b)] \right|;\ r_0 = \sqrt{R_b^{\,2} + a^2} \qquad (3.2)$$

Where P_{near} is the near-field pressure; k_w is the wavenumber ($k=2\pi F_0 C_s^{-1}$, F_0 is the ADP frequency and C_s is the speed of sound); and a is the transducer radius. This formula takes into account destructive and constructive interference between sound rays produced by the transducer.

The near-field correction for the 0.5 MHz instruments appears to have been successful. Figure 2.4 is typical for the 0.5 MHz instrument-there is a smooth, monotonic change in ABS with distance from the head. Despite the application of the near field correction, both 1.50 MHz instruments showed a characteristic minimum at the point where near-field effects should end and far-field effects (absorption and beam spreading) begin to dominate. The fact the both slant and vertical beams showed (for the two 1.5 MHz ADPs) a similar interference pattern tends to exclude as a cause systematic interference between beams or with instrument frame. The near-field correction for the 1.5 MHz instrument appears to need modification. Specifically, it is likely that the manufacturer has not defined the effective diameter of the transducer correctly. The Sontek ADP uses a "clamped" transducer to eliminate side band transmission, so the effective diameter is less than the actual diameter. Given the rather small diameter of a

1.5 MHz transducer, even a small error in diameter can cause significant uncertainty in near-field correction.

Each of the moored ADPs was calibrated against cruise SPM data from OBS. For the two 0.5 MHz three-beam ADPs instruments a single, slant beam was used. ABS from the vertical beam was used for the two four-beam instruments. An example calibration plot at Tansy during the May cruise is depicted in Fig. 3.1. A calibration plot for Am169 during the October cruise is shown in Fig 3.2. The regression lines for ABS vs. SPM for all stations ranged in slope from 0.90 to 1.09 mg $(l \times dB)^{-1}$. R^2 values ranging between 0.40 and 0.60 were obtained. Some of the scatter was probably due to the distance of the OBS from the ABS (usually between 50 and 100 meters). Differences in depth between the OBS sampling and moored instrument locations may also have caused differences in their respective profiles.

3.3 Inverse Analysis Details and Verification

The inverse analysis procedure employed provided us with detailed information on W_s-class distribution throughout the time record. That is, it optimally converted the observed ABS profile into profiles of the four pre-determined W_s-classes described in section 2.4.4. The inverse analysis was implemented as a non-negative least-squares (NNLS) method (Lawson and Hanson, 1974; Menlke 1989; Lynch and Agrawal, 1994; Shen and Lemmin, 1998). The profiles for the individual W_s-classes for each time and mooring were determined using a modified Rouse balance (Section 2.4.5). While the value of W_s is fixed for each W_s-class, the Rouse number P_i varies with time and location according to the local bedstress.

A comparison between moored ADP data and Owen Tube data was used to check the accuracy of our results (Table 3.3). Table 3.3 displays the mean Owen Tube concentrations in relationship to the moored ADP W_s-class overall results. There is close

agreement between the Owen Tube and the inverse analysis regarding the total near bed percentage of fines ($C_1 + C_2$) and aggregates plus sand ($C_3 + C_4$). There is also good individual agreement for the classes C_1 and C_2. This close agreement between the Owen Tube and the inverse analysis for the fine settling classes likely affects the relatively uniform distribution in the vertical of C_1 and C_2. The inverse analysis over-estimates the amount of C_4, even though the bottom ADP bin is above the minimal Owen Tube. There are several possible reasons for this disagreement for classes C_3 and C_4: a) uncertain and variable Owen Tube depth, especially during periods of strong currents when C_3 and C_4 concentrations are large, b) systematic bias produced by the presence of both sand and aggregates in C_4, c) uncertainties in the near-field corrections for the ABS (Fig. 2.4 and Fig. 2.5a), and d) size dependent acoustic response in the near Rayleigh scattering regime.

The sensitivity of the inverse analysis method was extensively tested using different choices for and numbers of W_s-classes. Use of two W_s classes with very similar characteristic profiles (determined by P_i) tended to result in zero values for one or the other W_s-class through most of the time record. Alternatively, the NNLS became unstable and failed to yield any results. Therefore, it was important to choose W_s-classes that had unique characteristic profiles. Initially three characteristic settling velocity classes were used. Closer examination of seasonal Owen Tube analysis showed four W_s-classes characterized the Columbia River estuary sediment most accurately. If three W_s-classes were used and the water column actually had more characteristic classes, analysis showed that the concentration in various classes would be less accurate. The use of five W_s-classes resulted in one of the classes almost always being zero. Four characteristic classes were used in the final analyses because this matched the cruise Owen Tube data most accurately provided physically reasonable results, as well as previous studies of sediment in the Columbia River Estuary (Gelfenbaum, 1983; Sherwood and Creager, 1990)

It was concluded that:

- The actual value of W_s for C_1 is unimportant, so long as it is small enough that the profile is essentially independent of z for all but the quietest flow conditions. This is achieved with a value of $W_s < 0.1$ mm s^{-1}.
- It was vital to include a W_s-class representative of the fastest settling material, because variance would otherwise be lost at the bed or the concentrations throughout the water column would be overestimated.
- The W_s-classes used in the inverse analysis should match the Owen tube-derived size spectrum, with adjacent W_s values differing by a factor of 5 to 10. If the W_s values are too closely spaced, the inverse analysis may become unstable because adjacent W_s-classes are almost redundant.

3.4 Summary

The correction and calibration of ABS and OBS is essential for accurate measurements of SPM concentrations. ABS profiles were corrected for sound and water absorption, beam spreading, and near-field effects. All backscatter was calibrated against SPM samples to provide total SPM concentration data. Comparisons were done between different choices for and numbers of W_s-classes, which resulted in the use of four characteristic W_s-classes (C_1-C_4). Non-negative least squares analysis was done for all moored ADP stations during the 9 month study period, providing information on sediment distribution and bulk sediment in and in the vicinity of the ETM.

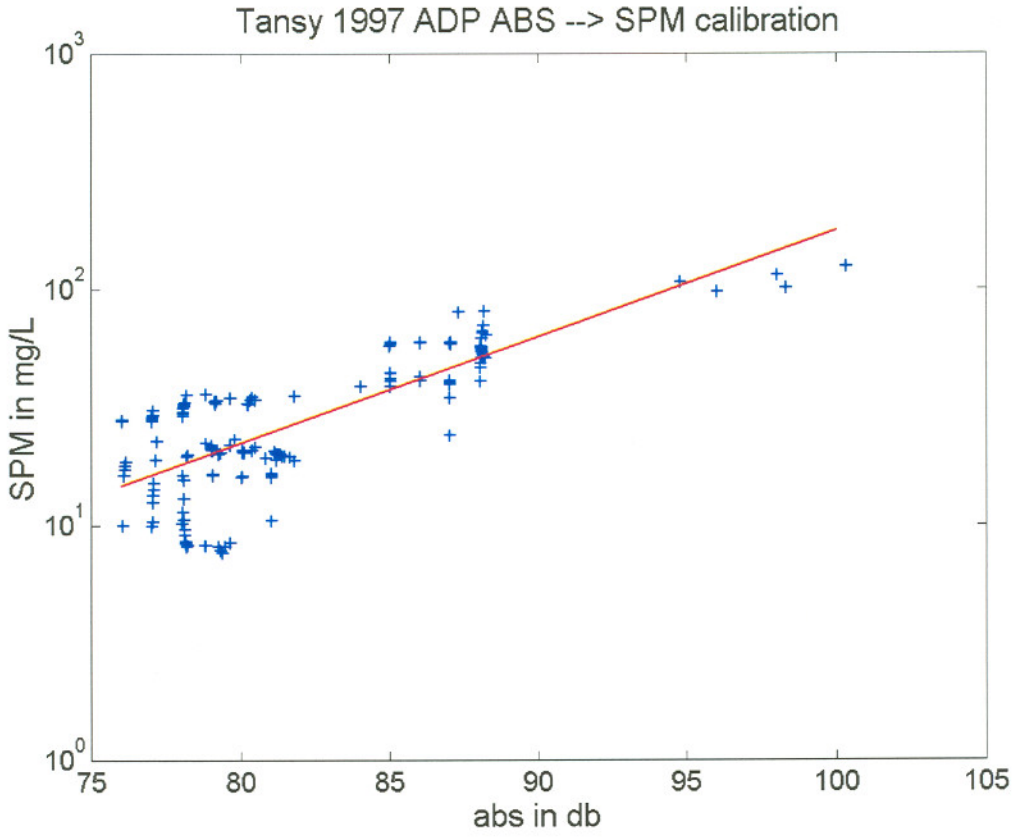

Figure 3.1. Calibration of ABS vs. SPM for May at Tansy point; R^2=0.60, $SPM=10^{0.0451(abs)-2.26}$.

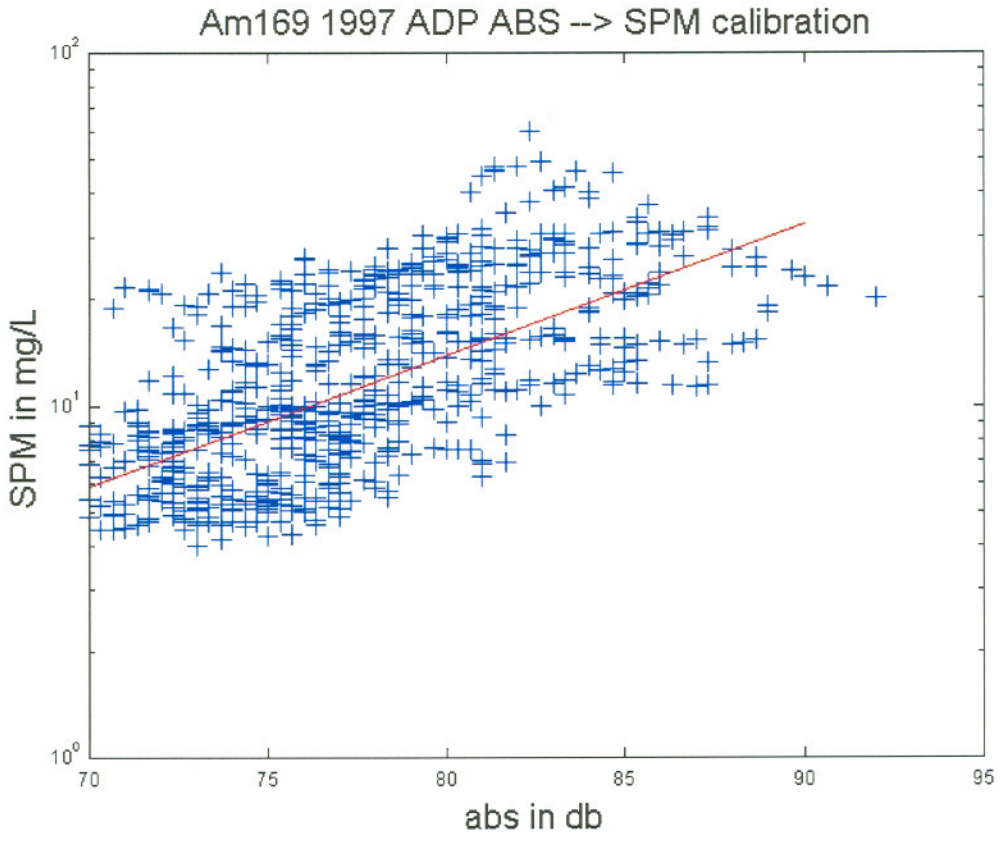

Figure 3.2. Calibration of ABS vs. SPM for October at Am169; R^2=0.40, $SPM=10^{0.037(abs)-1.82}$.

Table 3.1. Calibration of OBS vs. SPM for the three 1997 seasonal cruises.

Month of cruise	number of sample points	slope	spm intercept	R^2
May	129	1.84	0.227	0.882
July	172	2.13	-24.0	0.864
October	100	1.82	6.74	0.923

Table 3.2. Sound absorption values, coefficient α, for CORIE ADP's for three salinities and two frequencies.

Acoustic frequency	Absorption at sal=0	Absorption at sal=5	Absorption at sal=35
500 kHz	0.07 dB/meter	0.08 dB/meter	0.14 dB/meter
1500 kHz	0.60 dB/meter	0.61 dB/meter	0.67 dB/meter

Table 3.3. Owen Tube percentage size class comparison with moored ADP records.

Instrument /Station	Ws 0.014 mms^{-1}	Ws 0.30 mms^{-1}	Ws 2.0 mms^{-1}	Ws 14.0 mms^{-1}	Collection period
Owen tube (mean %)	4.4	26.4	35.6	34.2	May, July, & Oct cruises
CORIE stations (mean %)	2.5	28.3	24.0	45.2	May-Dec
Red26 (mean %)	3.8	25.5	20.5	50.2	May-Dec
Tansy (mean %)	1.2	27.8	29.6	41.4	May-Dec
Am169 (mean %)	1.6	37.5	10.5	50.5	May-Dec
Am012 (mean %)	3.5	22.5	35.4	38.6	May-Dec
Owen Tube (mean %)	5.4	16.9	27.1	46.4	cruise ebb
Owen Tube (mean %)	3.7	22.8	38.2	31.4	cruise flood
Owen Tube (mean %)	2.3	17.0	37.3	40.7	cruise spring
Owen Tube (mean %)	6.3	26.0	34.6	26.3	cruise neap

CHAPTER 4

Conclusions and Future Considerations

The year of this study, 1997, had a large spring freshet due to the effects of La Nina, causing large sediment transport, tides, and currents. Distinct neap-spring and seasonal fluctuations were observed in the low-pass filtered bulk sediment concentration, along-channel velocity, transport calculations, and concentrations of all W_s-classes at four moored CORIE ADPs. The major driving parameters, fluvial and tidal, were compared to differential advection. Rouse number (P), Advection number (A), and Trapping Efficiency (E) were determined to help understand patterns of sediment dynamics in various spatial and temporal regimes.

Suspended particulate matter in the Columbia River estuary ETM responds to changes in supply and external hydrodynamic forcing (tides and river flow) on a variety of time scales, from tidal to interannual. Sediment concentrations in the ETM were larger in the spring freshet than during the summer and fall seasons. During the freshet season spring tides at each station, a large export of SPM occurred. Both the mean outflow and tidal transport participated in this export at most stations. Net SPM transports were smaller during the rest of the year, with landward tidal transport being balanced by seaward mean flow transport at some stations. At other stations, the division between landward and seaward transport was a function of depth rather than mechanism; transport at the bed was landward, while near-surface transport was seaward. Advection was more prominent during neap tides, because of salt-wedge advection on flood and the slow erosion of salinity on ebb in the ETM region. Flood ETM events were more advective than ebb events, especially during spring-freshet neap tides. Trapping efficiency was

maximal during the lowest flow periods and exhibited significant spatial heterogeneity. Residence times calculations indicate the peripheral bays probably serve as important reservoirs for storage of SPM. The extensive cruise and moored instrument data and new inverse analysis procedure provide dynamical insight into ETM processes in the Columbia River Estuary.

Future studies should include effects of acceleration and advection in the equations of motion, as well as more sediment characterization data. Other determinations of sediment size by a Laser In-Situ Scattering and Transmissometry (LISST) instrument and video camera could enhance the instrument calibration. Additionally, the conversion of ABS to SPM by settling class using joint co-located optical-acoustic data could improve future calibrations by providing a dual frequency determination of sediment concentrations.

CHAPTER 5

References

Allen, G.P., J.C. Salomon, P. Bassoullet, Y. Du Pehoat, and C. De Grandpre. 1980. Effects of tides on mixing and suspended sediment in macrotidal estuaries. *Sedimentary Geology* 26: 69-80.

Ashjian, C.J., S.L. Smith, C.N. Flagg, C. Wilson. 1998. Patterns and occurrence of diel vertical migration of zooplankton biomass in the Mid-Atlantic Bight described by an acoustic Doppler current profiler. *Continental Shelf Research* 18: 831-858.

Baptista, A.M. 2000. *CORIE*. http://www.ccalmr.ogi.edu/CORIE/. Date viewed: June 15, 2000.

Baptista, A.M., M. Wilkin, P. Pearson, P. Turner, C. McCandlish, and P. Barrett. 1999. Coastal and Estuarine Forecast Systems: A Multi-Purpose Infrastructure for the Columbia River. *Earth System Monitor* 9(3): 1-5.

Baptista, A.M., M. Wilkin, P. Pearson, P. Turner, C. McCandlish, P. Barrett, S. Das, W. Sommerfield, M. Qi, N. Nangia, D. Jay, D. Long, C. Pu, J. Hunt, Z. Yang, E. Myers, J. Darland and A. Farrenkopf. 1998. Towards a Multi-Purpose Forecast System for the Columbia River Estuary. *Ocean Community Conference '98*, Baltimore, MD. pp. 1-6.

Barans, C.A., B.W. Sterner, D.V. Holliday, and C.F. Greenlaw. 1997. Variation in the vertical distribution of zooplankton and fine particles in an estuarine inlet of South Carolina. *Estuaries* 20(3): 487-482.

Baross, J. A., B. Crump, and C. A. Simenstad. 1994. Elevated 'microbial loop' activities in the Columbia River estuary turbidity maximum. In *Changes in Fluxes in Estuaries*, K.R. Dyer and R.J. Orth, eds, Frendesborg, Denmark: Olsen and Olsen. pp. 459-464.

Battisto, G.M., C.T. Friedrichs, H.C. Miller, D.T. Resio. 1999. Response of OBS to mixed grain size suspension during SandyDuck '97. In *Proceedings of the 4th*

International Symposium on Coastal Engineering and Science of Coastal Sediment Processes, N.C. Kraus and W.G. McDougal, eds. pp. 258-263.

Beach, R.A. and R.W. Sternberg. 1988. Suspended sediment transport in the surf zone: response to cross-shore infragravity motion. *Marine Geology* 80: 61-79.

Bokuniewicz, H. and C.L. Arnold. 1984. Characteristics of suspended sediment transport in the lower Hudson River. *Northeastern Environmental Science* 3: 184-189.

Callaway, R.J. 1971. Application of some numerical models to Pacific Northwest estuaries. In *Technical Conference on Estuaries of the Pacific Northwest*, Nath, J.N. and L.S. Slotta, eds. pp. 29-97.

Clay C.S. and H.M. Medwin. 1977. *Acoustical Oceanography*. New York, NY: John Wiley and Sons.

Crawford, A.M. and A. Hay. 1993. Determining suspended sand size and concentration from multifrequency acoustic backscatter. *Journal of Acoustical Society of America* 94(6): 3312-3324.

CREST. 1984. *Sedimentary Processes and Environments in the Columbia River Estuary*. Astoria, OR: CREST.

CRETM-LMER. 2000. *CRETM-LMER More information*. http://depts.washington.edu/cretmweb/moreinfo.html. Date viewed: June 15, 2000.

Crump, B.C. and J.A. Baross. 1996. Particle-attached bacteria and heterotrophic plankton associated with the Columbia River estuarine turbidity maxima. *Marine Ecology Progress Series* 138: 265-273.

Deines, K. 1999. Backscatter estimation using broadband acoustic doppler current profilers. In *Proceedings of the IEEE Sixth Working conference on current Measurement*, S.P. Anderson, E.A. Terray, J.A. Rizoli White, and A. J. Williams, III, eds, March 11-13, 1999, Piscataway, NJ: IEEE. pp. 249-253.

Downing, A., P.D. Thorne, and C.E. Vincent. 1995. Backscattering from a suspension in the near field of a piston transducer. *Journal of Acoustical Society of America* 97(3): 1614-1620.

Drake, D.E. and D.A. Cachione. 1989. Estimate of the suspended sediment reference concentration (C_a) and resuspension coefficient (γ_0) from near-bottom observations on the California shelf. *Continental Shelf Research* 9(1): 51-64.

Flagg, C.N. and S.L. Smith. 1989. On the use of the acousitc Doppler current profiler to measure zooplankton abundance. *Deep-Sea Research* 36(3): 455-474.

Fredsoe, J. and R. Deigaard. 1992. *Mechanics of Coastal Sediment Transport*. Singapore: World Scientific.

Gelfenbaum, G. 1983. Suspended-sediment response to semidiurnal and fortnightly tidal variations in a mesotidal estuary: Columbia River, USA. *Marine Geology* 52: 39-57.

Giese, B.S and D.A. Jay. 1989. Modeling tidal energetics of the Columbia River Estuary. *Estuaries, Coastal and Shelf Science* 29: 549-571.

Glenn, S.M. and W.D. Grant. 1987. A suspended sediment stratification correction for combined wave and current flows. *Journal of Geophysical Research* 92(C8): 8244-8264.

Grabemann, I. and G. Krause. 1989. Transport processes of suspended matter derived from time series in a tidal estuary. *Journal of Geophysical Research* 94(C10): 14373-14379.

Green, M.O., R.G. Bell, T.J. Dolphin, A. Swales. 2000. Silt and sand transport in a deep tidal channel of a large estuary (Manukau Harbour, New Zealand). *Marine Geology* 163: 217-240.

Hamblin, P.F. 1989. Observations and model of sediment transport near the turbidity maximum of the Upper Saint Lawrence Estuary. *Journal of Geophysical Research* 97 (C10): 14419-14428.

Hamilton, L.J. 1998. Calibration and interpretation of acoustic backscatter measurements of suspended sediment concentration profiles in Sydney Harbour. *Acoustics Australia* 26(3): 87-93.

Hamilton, L.J., Z. Shi, and S.Y. Zhang. 1998. Acoustic backscatter measurements of estuarine suspended cohesive sediment concentration profiles. *Journal of Coastal Research* 14(4): 1213-1224.

Hanes, D.M., C.E. Vincent, D.A. Huntley, and T.L Clarke. 1988. Acoustic measurements of suspended sand concentration in the C^2S^2 experiment at Stanhope Lane, Prince Edward Island. *Marine Geology* 81: 185-196.

He, C. and A.E. Hay. 1993. Broadband measurements of the acoustic backscatter cross section of sand particles in suspension. *Journal of Acoustical Society of America* 94(4): 2247-2254.

Holdaway, G.P. and P.D. Thorne. 1997. Determination of a fast and stable algorithm to evaluate suspended sediment parameters from high resolution acoustic backscatter systems. In *7th International Conference on Electronic Engineering in Oceanography*, Piscataway, NJ: IEEE. pp. 86-92.

Hughes, F.W. and M. Rattray. 1980. Salt flux and mixing in the Columbia River estuary. *Estuarine and Coastal Marine Science* 10: 479-492.

Jay, D.A., W.R. Geyer and D.R. Montgomery. 2000. An ecological perspective on estuarine classification. In *Estuarine Science, A Synthetic Approach to Research and Practice,* J.E. Hobbie, ed, Washington DC: Island Press. pp. 149-176.

Jay, D.A. and J.D. Musiak. 1994. Particle trapping in estuarine tidal flows. *Journal of Geophysical Research* 99(C10): 20445-20461.

Jay, D.A. and J.D. Musiak. 1996. Internal Tidal Asymmetry in Channel Flows: Origins and Consequences. In *Mixing in Estuaries and Coastal Seas*, C. Pattiaratchi ed, Washington DC: AGU. pp. 211-249.

Jay, D.A. and P. Naik. 2000. Climate effects on Columbia River sediment transport. In *Southwest Washington Coastal Erosion Workshop Report 1999*, US Geological Survey Open File Report, G. Gelfenbaum and G. Kaminsky, ed, (submitted).

Jay, D.A., P. Orton, D.J. Kay, A. Fain, and A.M. Baptista. 1999. Acoustic determination of sediment concentrations, settling velocities, horizontal transports and vertical fluxes in estuaries. In *Proceedings of the IEEE Sixth Working Conference on Current Measurement*, S.P. Anderson, E. A. Terray, J.A. Rizoli White, and A. J. Williams, III, eds, March 11-13, 1999, Piscataway, NJ: IEEE. pp. 258-263.

Jay, D.A. and J.D. Smith. 1990. Circulation, density distribution and neap-spring transitions in the Columbia River Estuary. *Progress in Oceanography* 25: 81-112.

Kay, D. J., D.A. Jay and J.D. Musiak. 1996. Salt transport through an estuarine cross-section calculated from moving vessel ADCP and CTD data Buoyancy Effects on Coastal and Estuarine Dynamics. In *Buoyancy Effects on Coastal and Estuarine Dynamics*, D.G. Aubrey and C. Friedrichs, eds, Washington DC: AGU. pp. 195-212.

Kaiser, J.F. 1974. Non-recursive digital filter design using the lo-sinh window function. In *Proceedings of 1974 IEEE Symposium on Circuits and Systems*, Piscataway, NJ: IEEE. pp. 20-23.

Kineke, G.C. and R.W. Sternberg. 1989. The effect of particle settling velocity on computed suspended sediment concentration profiles. *Marine Geology* 90: 159-174.

Kineke, G.C. and R.W. Sternberg. 1992. Measurements of high concentration suspended sediments using the optical backscatterance sensor. *Marine Geology* 108: 253-258.

Lawson, C.L. and R.J. Hanson. 1974. *Solving Least Square Problems*. Englewood Cliffs, New Jersey: Prentice-Hall.

Lee, H.L. and D.M. Hanes. 1995. Direct inversion method to measure the concentration profile of suspended particles using backscattered sound. *Journal of Geophysical Research* 100(C2): 2649-2657.

Lee, H.L. and D.M. Hanes. 1996. Comparison of field observations of the vertical distribution of suspended sand and its prediction by models. *Journal of Geophysical Research* 101(C2): 3561-3572.

Libicki, C., K. Bedford, and J. Lynch. 1989. The interpretation and evaluation of a 3-MHz acoustic backscatter device for measuring benthic boundary layer sediment dynamics. *Journal of Acoustical Society of America* 85(4): 1501-1511.

Long, C.E. 1981. *A simple model for time-dependent stably stratified turbulent boundary layers*. Ph.D Thesis. Seattle, WA: University of Washington, Department of Oceanography.

LMER Coordinating Committee (Boynton, W., J.T. Hollibaugh, D. Jay, M. Kemp, J. Kremer, C. Simenstad, S.V. Smith, and I. Valiela). 1992. Understanding changes in coastal environments: the Land Margin Ecosystems Research Program. *EOS* 73: 481-485.

Lucas, L.V., J.K. Thompson, J.R. Koseff, and S.B. Monismith. 1999. Processes governing phytoplankton bloom in estuaries--Part I, The role of horizontal transport. *Marine Ecology Progress Series* 187: 1-16.

Ludwig, K.A. and D.M. Hanes. 1990. Laboratory evaluation of optical backscatterance suspended solids sensors exposed to sand-mud mixtures. *Marine Geology* 94: 173-179.

Lynch, J.F. 1985. Theoretical analysis of ABSS data for Hebble. *Marine Geology* 66: 277-289.

Lynch, J.F. and Y.C. Agrawal. 1991. A model-dependent method for inverting vertical profiles of scattering to obtain particle size spectra in boundary layers. *Marine Geology* 99: 387-401.

Lynch, J.F., T.F. Gross, B.H. Brumley, and R.A. Filyo. 1991. Sediment concentration profiling in HEBBLE using a 1-MHz acoustic backscatter system. *Marine Geology* 99: 361-385.

Lynch, J.F., J.D. Irish, C.R. Sherwood, and Y.C. Agrawal. 1994. Determining suspended sediment particle size information from acoustical and optical backscatterance measurements. *Continental Shelf Research* 14(10/11): 1139-1165.

Menlke, W. 1989. *Geophysical Data Analysis: Discrete Inverse Theory*. London: Academic Press.

Middleton, G.V. and J.B. Southard. 1984. *Mechanics of Sediment Movement.* Tulsa, OK: Society of Economic Paleontologists and Mineralogists.

Morgan, C.A., J.R. Cordell, and C.A. Simenstad. 1997. Sink or swim? Copepod population maintenance in the Columbia River estuarine turbidity maxima region. *Marine Biology* 129: 309-317.

Nichols, M.M. and R.B. Biggs. 1985. Estuaries. In *Coastal Sedimentary Environments*, Davis R.A., Jr., ed, New York, NY: Springer-Verlag. pp. 77-186.

Nowell, A.R.M. 1983. The benthic boundary layer and sediment transport. *Reviews in Geophysics and Space Physics* 21: 1181.

Nowell, A.R.M. and C.E. Long. 1983. An evaluation of Von Karman's constant. In *Pollutant Transfer and Sediment Dispersal in the Washington Oregon Coastal Zone: Report of Progress, 1 August 1982-31 July 1983*, B. Hickey, ed, Seattle, WA: University of Washington.

Orton, P.M. 1996. *Evaluation of the Applicability of Vertical Suspended Sediment Distribution Equations in an Estuarine Turbidity Maximum.* Master's thesis. Columbia, SC: University of South Carolina.

Osborne, P.D., C.E. Vincent, and B. Greenwood. 1994. Measurement of suspended sand concentrations in the nearshore: field intercomparison of optical and acoustic backscatter sensors. *Continental Shelf Research* 14(2/3): 159-174.

Reed, D.J. and J. Donovan. 1994. The character and composition of the Columbia River estuarine turbidity maximum. In *Changes in fluxes in Estuaries*, K.R. Dyer and R.J. Orth, eds, Fredensborg, Denmark: Olsen and Olsen. pp. 445-450.

Schaffsma, A.S. and A.E. Hay. 1997. Attenuation in suspensions of irregularly shaped sediment particles: A two-parameter equivalent spherical scatterrer model. *Journal of Acoustical Society of America* 102 (3): 1485-1502.

Shen C. and U. Lemmin. 1998. Improvements in acoustic sediment concentration profiling using an LMS compensation algorithm. *IEEE Journal of Oceanic Engineering* 23(2): 96-104.

Sherwood, C.R. and J.S. Creager. 1990. Sedimentary geology of the Columbia River Estuary. *Progress in Oceanography* 25: 15-79.

Sherwood, C.R., D.A. Jay, R.B. Harvey, P. Hamilton, and C.A. Simenstad. 1990. Historical changes in the Columbia River Estuary. *Progress in Oceanography* 25: 299-352.

Shi, Z., L.F. Ren, and L.J. Hamilton. 1999. Acoustic profiling of fine suspension concentration in the Changjiang Estuary. *Estuaries* 22(3A): 648-656.

Simenstad, C.A., D.A. Jay, and C.R. Sherwood. 1992. Impacts of watershed management on land-margin ecosystems: the Columbia River Estuary as a case study. In *New Perspectives for Watershed Management - Balancing Long-term Sustainability with Cumulative Environmental Change*, R. Naimen, ed, New York, NY: Springer-Verlag. pp. 266-306.

Simenstad, C.A., D.J. Reed, D.A. Jay, J.A. Baross, F.G. Prahl and L.F. Small. 1994. Land-margin ecosystem research in the Columbia River estuary: investigations of the couplings between physical and ecological processes within estuarine turbidity maxima. In *Changes in fluxes in Estuaries*, K.R. Dyer and R.J. Orth, eds, Fredensborg, Denmark: Olsen and Olsen. pp. 437-444.

Simenstad, C.A., L.F. Small, C.D. McIntire, D.A. Jay, and C. Sherwood. 1990. Columbia River Estuary studies: An introduction to the estuary, a brief history, and prior studies. *Progress in Oceanography* 25: 1-13.

Smith, J.D. and S.R. McLean. 1977. Spatially averaged flow over a wavy surface. *Journal of Geophysical Research* 82(12): 1735-1746.

Smith, S.V., J.T. Hollibaugh, S.J. Dollar, and S. Vink. 1991. Tomales Bay metabolis: C-N-P stoichiometry and ecosystem heterotrophy at the land-sea interface. *Estuarine, Coastal and Shelf Science* 33: 223-57.

Sommerfield, W.N. 1999. *Variability of residual properties in the Columbia River Estuary: pilot application of emerging technologies*. Master's thesis. Portland, OR: Oregon Graduate Institute of Science and Technology.

Sontek Data Report. 1996. *ADP deployment near San Felipe, Mexico*. San Diego, CA: Sontek.

Sontek Technical Notes. 1997. *Acoustic Doppler Profiler (ADP) Principles of Operation*. San Diego, CA: Sontek.

Sontek Technical Notes. 1998. *Acoustical Doppler Profiler: Signal-Strength Correction*. San Diego, CA: Sontek.

Sternberg, R.W., I. Berhane, and A.S. Ogston. 1999. Measurement of size and settling velocity of suspended aggregates on the northern California continental shelf. *Marine Geology* 154: 43-53.

Thevenot, M.M. and N.C. Krauss. 1993. Comparison of acoustical and optical measurements of suspended material in the Cheasapeake Estuary. *Journal of Marine Environmental Engineering* 1: 65-79.

Thorne, P.D., C.E. Vincent, P.J. Hardcastle, S. Rehman, and N. Pearson. 1991. Measuring suspended sediment concentrations using acoustic backscatter devices. *Marine Geology* 98: 7-16.

USACE. 1999. *The Columbia-Snake River Basin*. http://www.nwd-wc.usace.army.mil/TMT/basin.html. Date viewed: June 20, 2000.

US Geological Survey. 1971. *Distribution of Radionuclides in Bottom Sediments of the Columbia River Estuary*. Portland, OR: US Department of the Interior.

US Geological Survey. 2000. *Historical Streamflow Daily Values for Columbia R At Beaver Army Terminal Nr Quincy,Ore* (14246900). http://waterdata.usgs.gov/nwis-w/OR/data.components/hist.cgi?statnum=14246900. Date viewed: May 15, 2000.

Vincent C.E. and M.O. Green. 1990. Field measurements of the suspended sand concentration profiles and fluxes and of the resuspension coefficient γ_0 over a rippled bed. *Journal of Geophysical research* 94(C7): 11591-11601.

Weir, D.J. and J. Mc Manus. 1987. The role of wind in generating turbidity maxima in the Tay Estuary. *Continental Shelf Research* 7: 1315-1318.

Winterwerp, J.C., J.M. Cornelisse, and C. Kuijper. 1993. A laboratory study on the behavior of mud from the Western Scheldt under tidal conditions. In *Nearshore and Estuarine Cohesive Sediment Transport*. Washington DC: AGU. pp. 295-313.

Wright, L.D. 1995. *Morphodynamics of Inner Continental Shelves*. Boca Raton, FL: CRC Press.

Young, R.A., J.T. Merrill, T.L. Clarke, J.R. Proni. 1982. Acoustic profiling of suspended sediments in the marine bottom boundary layer. *Geophysical Research Letters* 9(3): 175-178.

APPENDIX A

Along-channel velocity, total SPM, and W_s-class SPM for all CORIE ADPs

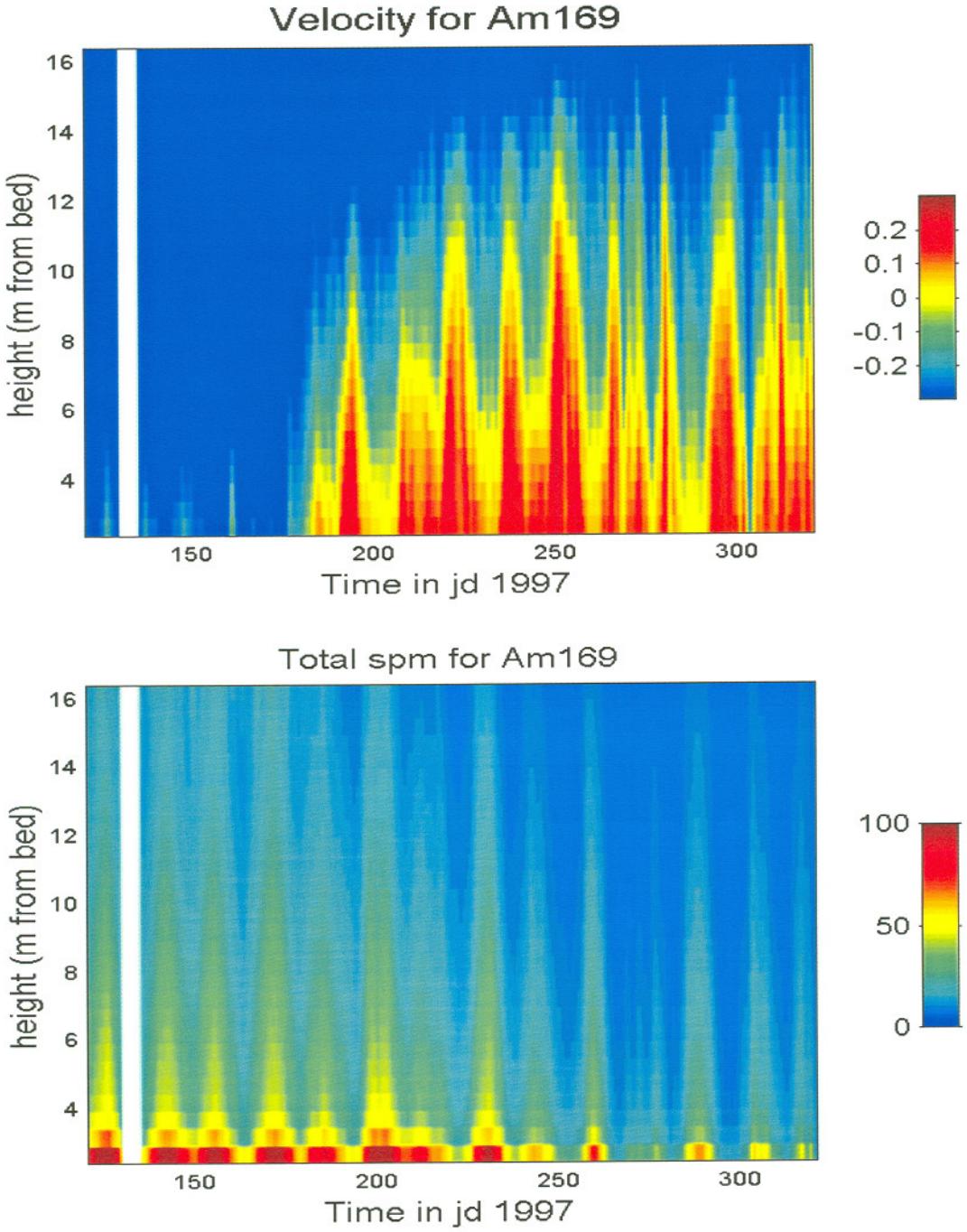

Figure A.1. Low pass filtered along-channel velocity (m s^{-1}) and low pass filtered total SPM (mg l^{-1}) at Am169 from May to December 1997. Both have been low pass filtered. Negative velocities are seaward.

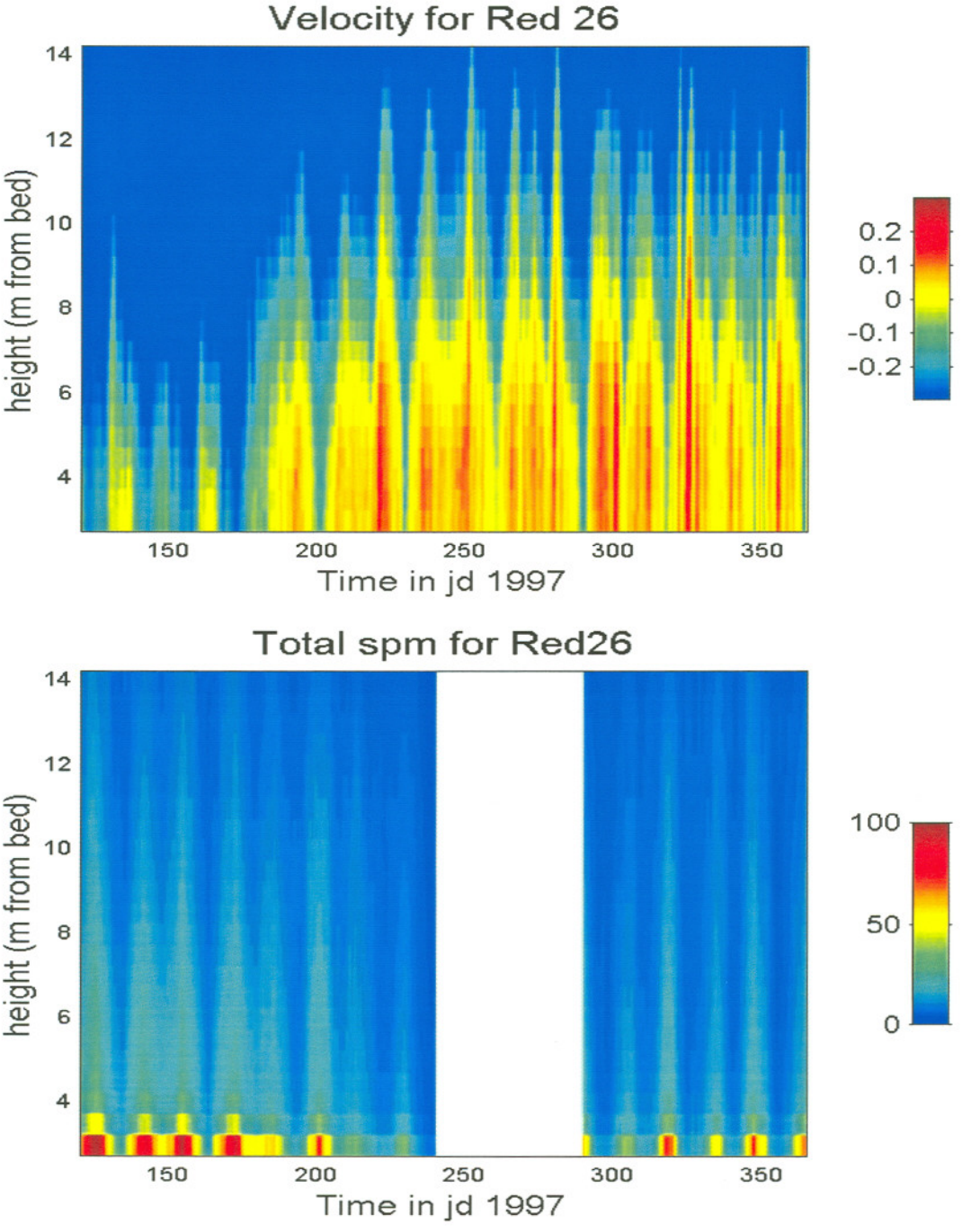

Figure A.2. Low pass filtered along-channel velocity (m s^{-1}) and low pass filtered total SPM (mg l^{-1}) at Red26 from May to December 1997. Both have been low pass filtered. Negative velocities are seaward.

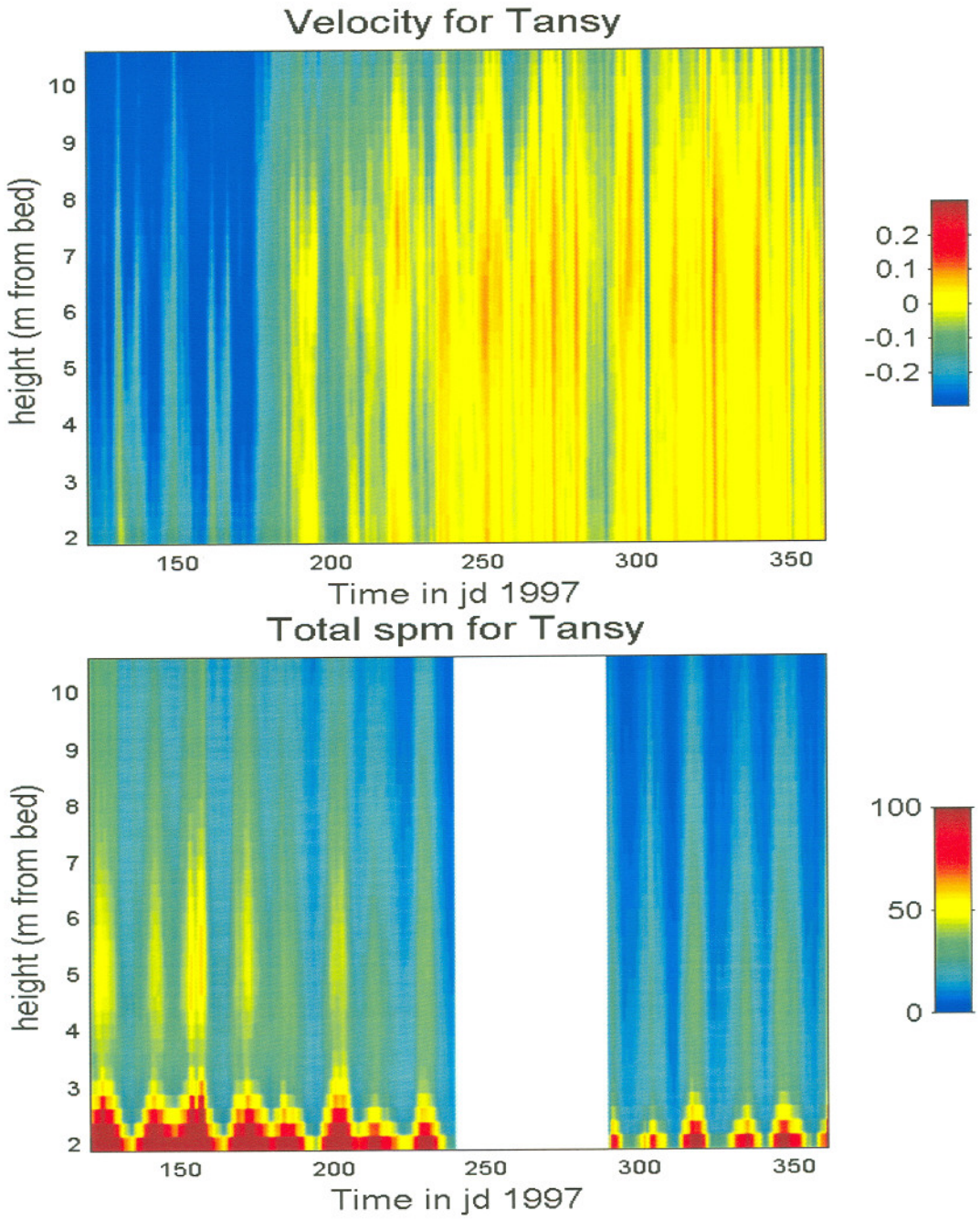

Figure A.3. Low pass filtered along-channel velocity (m s^{-1}) and low pass filtered total SPM (mg l^{-1}) at Tansy from May to December 1997. Both have been low pass filtered. Negative velocities are seaward.

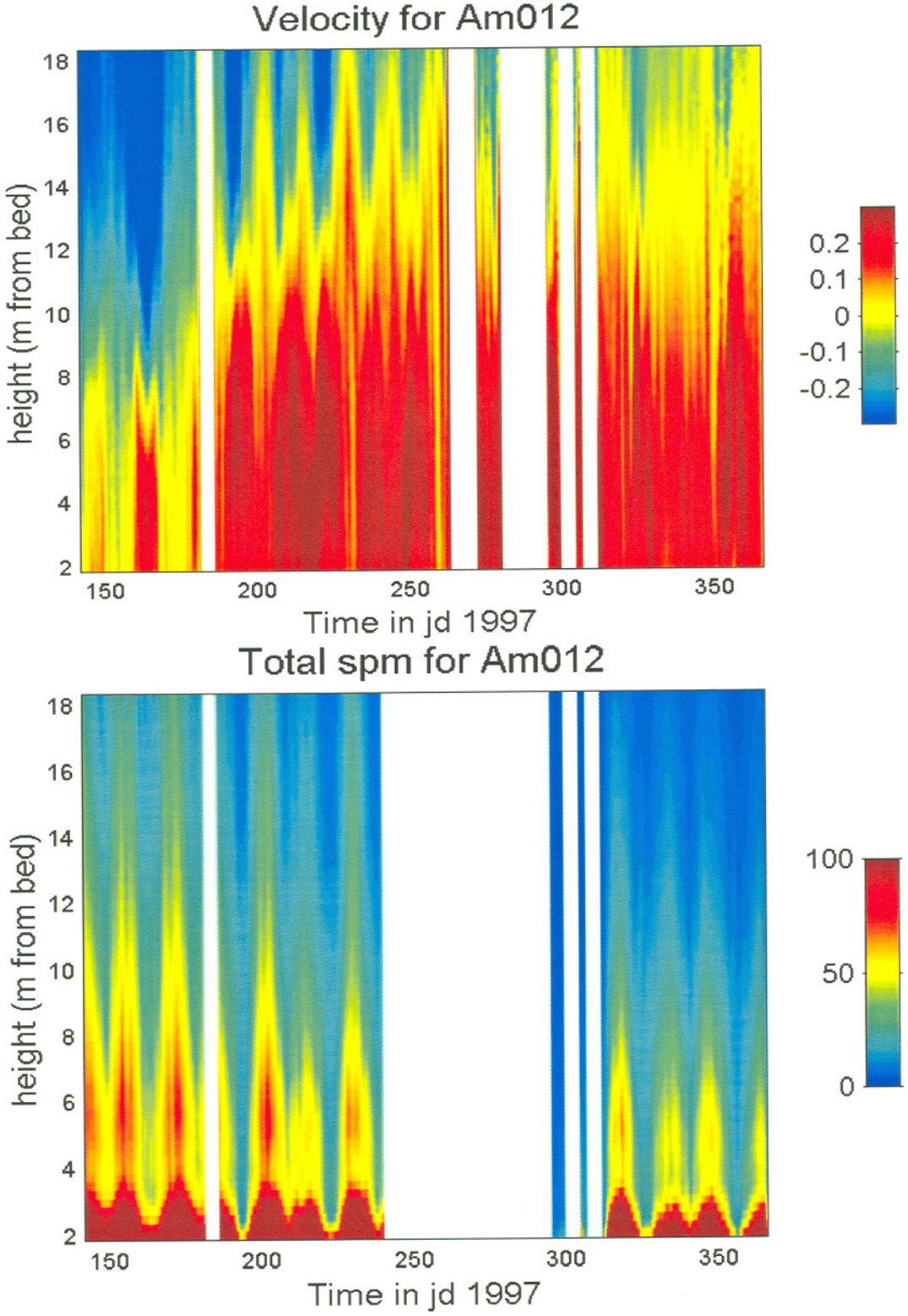

Figure A.4. Low pass filtered along-channel velocity (m s^{-1}) and low pass filtered total SPM (mg l^{-1}) at Am012 from May to December 1997. Both have been low pass filtered. Negative velocities are seaward.

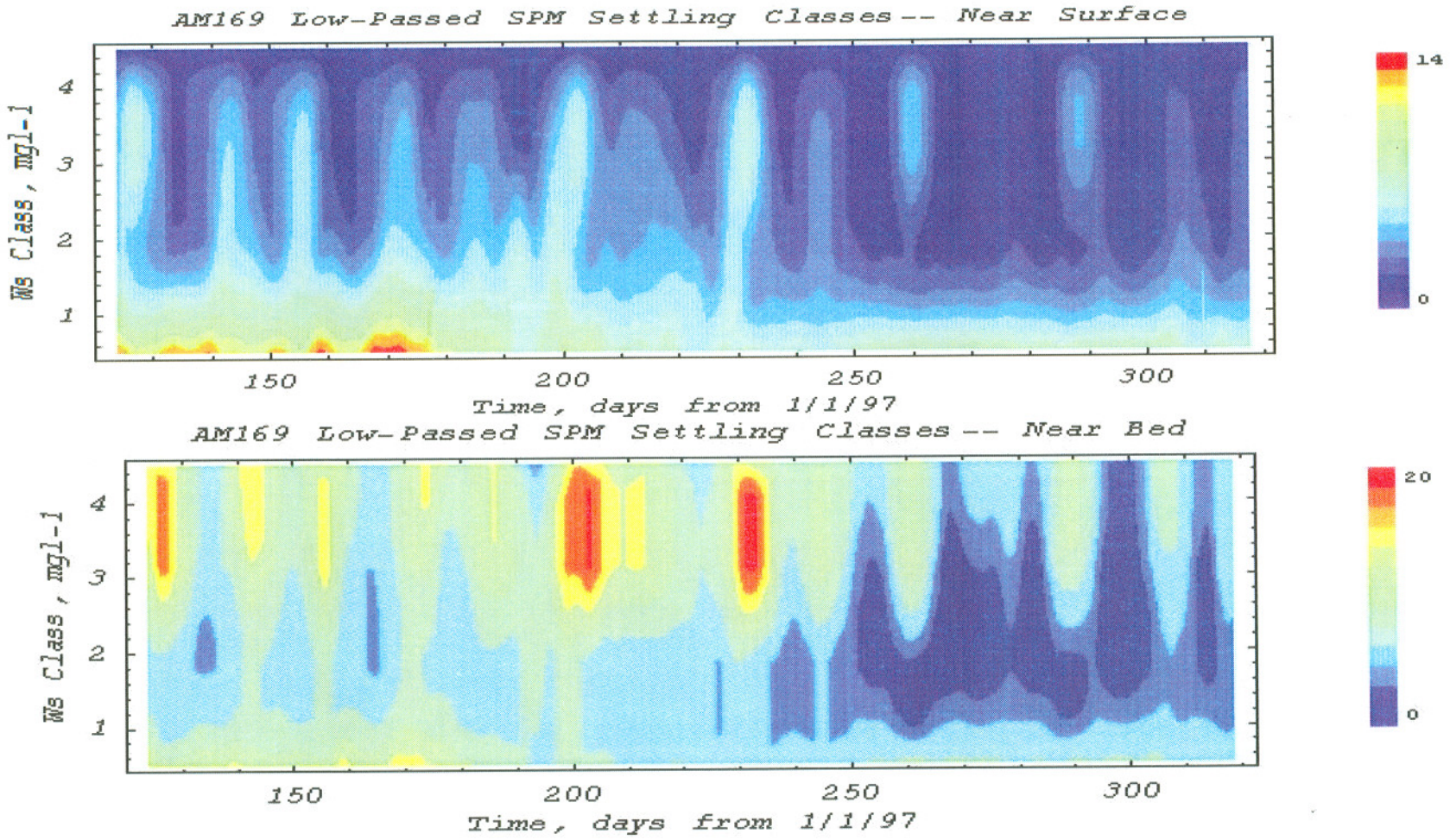

Figure A.5. Inverse analysis low pass filtered concentrations for all four W_s-classes at Am169, near the surface (a) and bed (b). Neap-spring fluctuations are evident in all settling classes, as well as seasonal variations. Sediment concentrations are in mg l^{-1}. The dark blue color indicates no data or no material found.

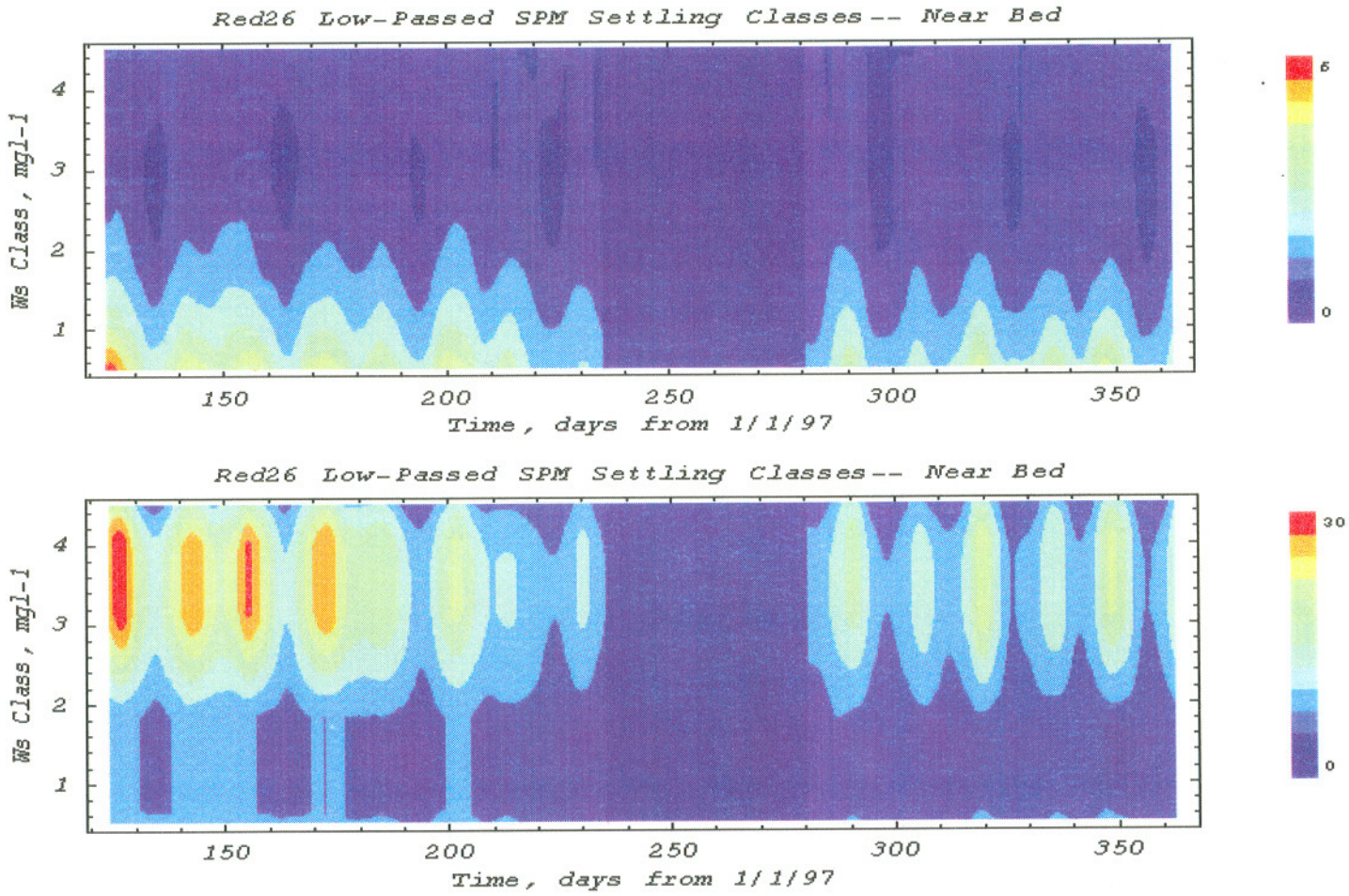

Figure A.6. Inverse analysis low pass filtered concentrations for all four W_s-classes at Red26, near the surface (a) and bed (b). Neap-spring fluctuations are evident in all settling classes, as well as seasonal variations. Sediment concentrations are in mg l^{-1}. The dark blue color indicates no data or no material found.

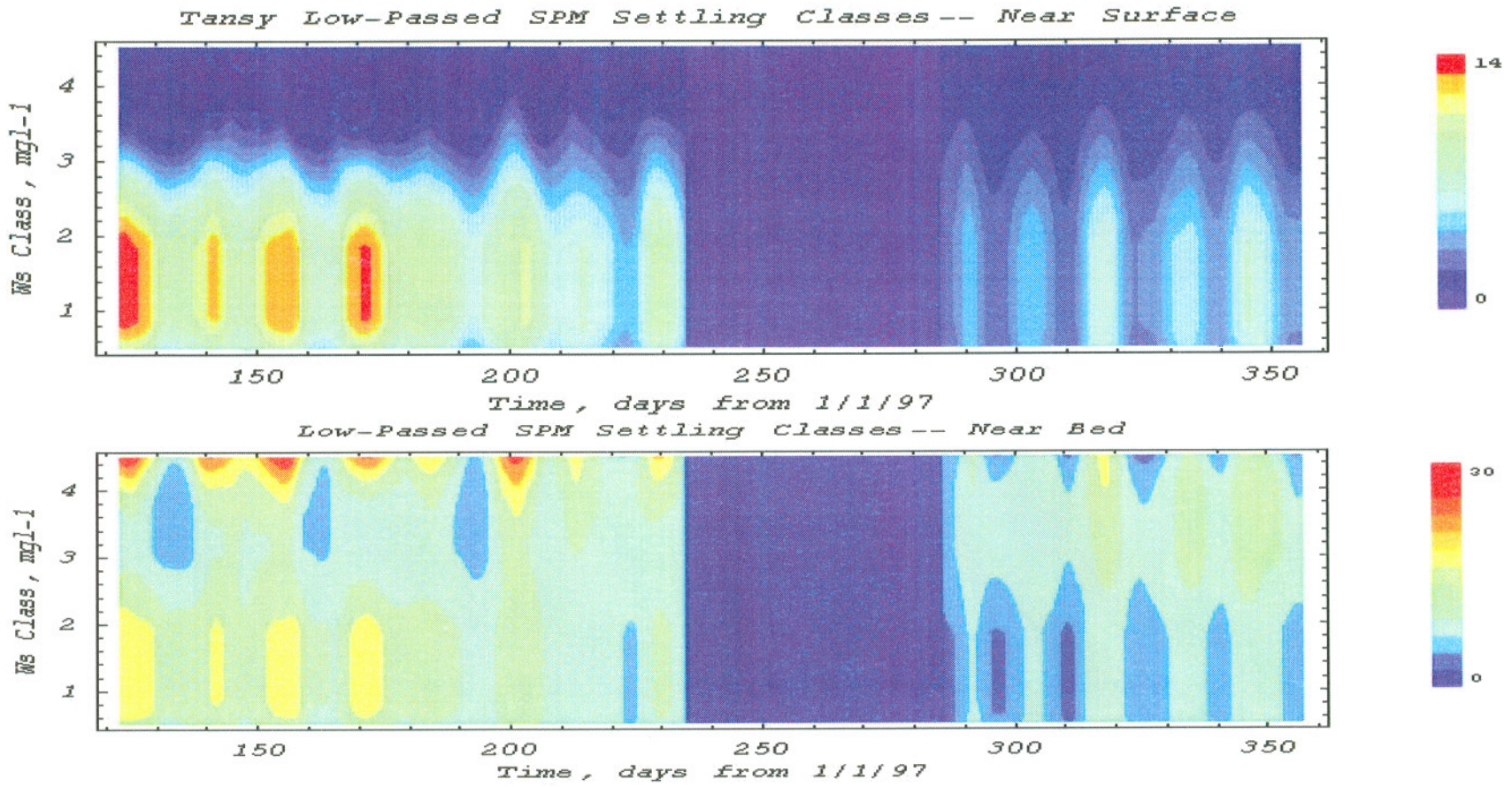

Figure A.7. Inverse analysis low pass filtered concentrations for all four W_s-classes at Tansy, near the surface (a) and bed (b). Neap-spring fluctuations are evident in all settling classes, as well as seasonal variations. Sediment concentrations are in mg l^{-1}. The dark blue color indicates no data or no material found.

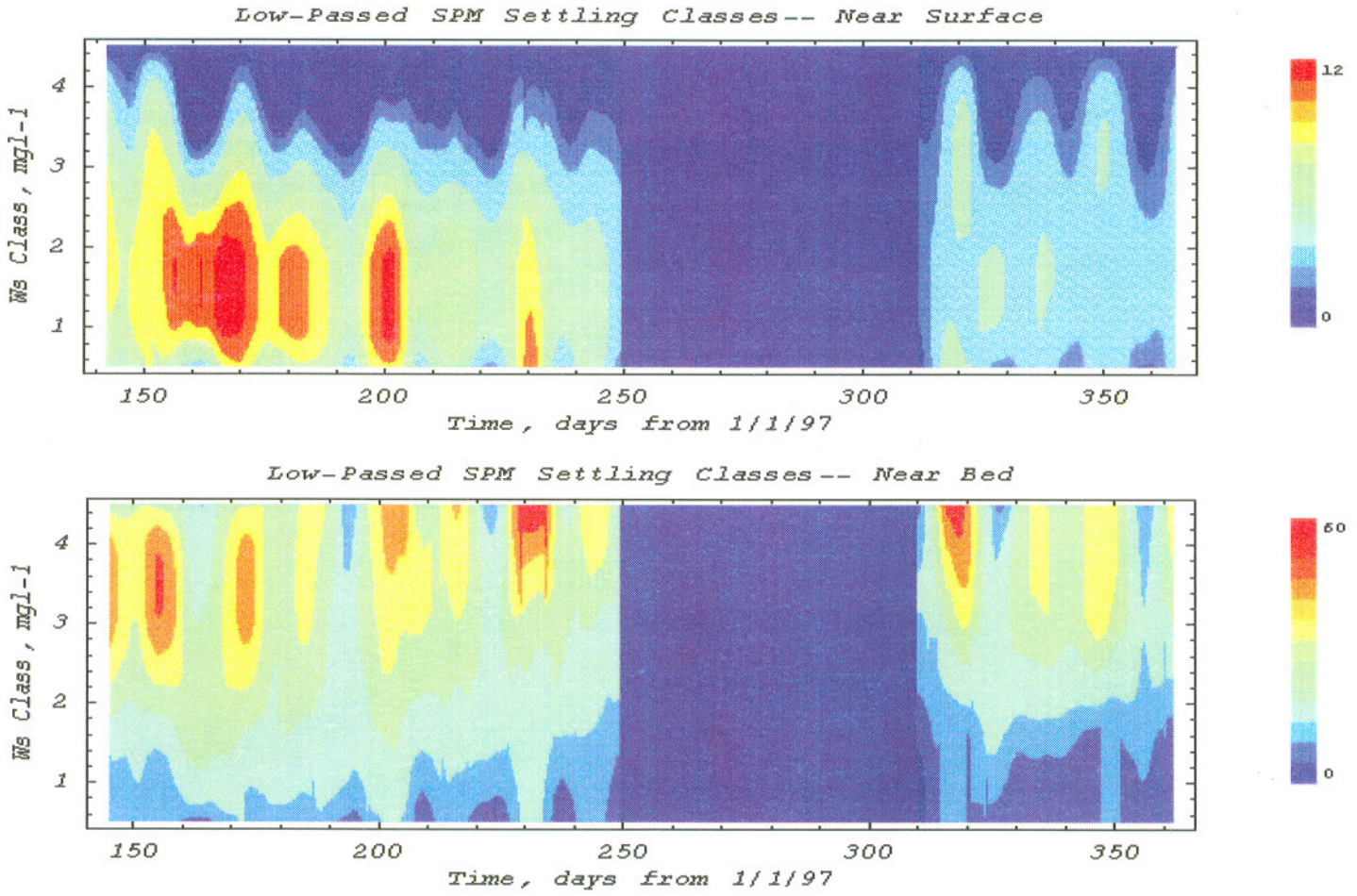

Figure A.8. Inverse analysis low pass filtered concentrations for all four W_s-classes at Am012, near the surface (a) and bed (b). Neap-spring fluctuations are evident in all settling classes, as well as seasonal variations. Sediment concentrations are in mg l^{-1}. The dark blue color indicates no data or no material found.

Biographical Sketch

I was born on April 9, 1975 in Seattle, WA. I graduated from Western Washington University in June 1997 with a Bachelor of Science degree in Environmental Science and a minor in Chemistry. After working as an environmental educator in Memphis, TN for a year, I moved back to the Northwest to continue my education.

In June 1997, I entered into the master's program at the Oregon Graduate Institute of Science and Technology and was awarded a Master of Science degree in Environmental Science and Engineering in October 2000. Over the past year I have had the opportunity to present my research at two estuarine conferences. I am looking forward to continuing studying water and sediment movement through the Ph.D. program at the University of Washington in the Marine Geology and Geophysics division of the Department of Oceanography.

Publication:

Jay, D.A., P. Orton, D.J. Kay, A. Fain, and A.M. Baptista. 1999. Acoustic determination of sediment concentrations, settling velocities, horizontal transports and vertical fluxes in estuaries. In *Proceedings of the IEEE Sixth Working Conference on Current Measurement*, S.P. Anderson, E.A. Terray, J.A. Rizoli White, and A.J. Williams, III, eds, March 11-13, 1999, Piscataway, NJ: IEEE. pp. 258-263.